UNIVERSITÀ DEGLI STUDI DI PALERMO

**DEPARTMENT OF EXPERIMENTAL BIOMEDICINE AND CLINICAL NEUROSCIENCES**

Ph.D. School of BIOMEDICINE AND NEUROSCIENCE, curriculum in Neuroscience

# THE ROLE OF HSP60 IN AMYLOID BETA PATHWAY: RELEVANCE TO ALZHEIMER'S DISEASE

**S. S. D. BIO/16**

**PhD Thesis of:**

**Claudia Marino**

***PROGRAM DIRECTOR:***

**Prof.ssa Felicia Farina**

***Tutor:***

***Prof. Giovanni Zummo***

***Co-Tutors:***

***Prof. Giulio Taglialatela***

***Dr. Pier Luigi San Biagio***

XXIX CYCLE
2017

DOTTORATO

*"…We apparently appear to have in front of us a peculiar disease process… we should not let ourselves to be satisfied with trying to include (…) any clinically unclear illness case into one of the diagnostic entities known to us"*
*-Alois Alzheimer-*

# *Table of Contents*

## *Disclosure*

- The following Research has been conducted in collaboration with the National Research Council, Department of Biophysics, Palermo and in collaboration with the University of Texas Medical Branch, Galveston, TX.

- Part of the Research has been extracted from the following publication:

*Mangione M.R., Vilasi S.,* ***Marino C.****, Librizzi F., Canale C., Spigolon D., Fucarino A., Passantino R., Cappello F., Bulone D. San Biagio P. L. (2016) Hsp60, amateur chaperon in amyloid-beta fibrillogenesis. BBA- General subjects 1860 (11): 2474-2483.*

## *Acknowledgments*

*I would like to particularly thank my mentor, Dr. Taglialatela, for guiding me and supporting me during these years of my PhD in USA, especially during the most challenging times.*
*I would like also to thank Dr. Taglialatela's laboratory for their precious advices, for sharing science and helping me in troubleshooting some of the experiments, particularly:*
*Dr. Balaji Krishan,*
*Wen-ru Zhang,*
*David Briley,*
*Michele Comerota,*
*Anna Fracassi,*
*Whitney Franklin,*
*Olga Zolochevzka,*
*Ayush Singh.*
*Dr. D.J. Selkoe for CHO and 7PA2 cell lines;*
*Dr. Randy Woltjer from the Oregon Brain Bank at Oregon Health and Science University (OHSU), for post mortem tissues,*
*Dr. Wood and Dr. Widen for helping me with the design of plasmids,*
*Dr. Maria Adelaide Micci for her maternal and professional support.*
*The UTMB Dean, Dr. David Niesel*
*Dr. Rakez Kayed*
*Dr. Yogesh Wairkar*
*Dr. Meli for precious discussions and help for troubleshooting*
*The NGP program Director, Dr. Owen Hamill*
*The NGP program coordinator, Aurora Galvan*
*Special thanks go to Prof. Francesco Cappello for guiding me during these three long years,*
*Prof. Giovanni Zummo*
*Dr. Antonella Marino Gammazza*
*I would also like to thank my co-mentor in Italy, Dr. Pier Luigi San Biagio for giving me the opportunity to do my first year of PhD at the Biophysics Institute at the National Research Institute, and all collaborators that helped and supported me during that year:*
*Dr. Donatella Bulone*
*Dr. Maria Rosalia Mangione,*
*Dr. Rosa Passantino*
*Dr. Silvia Vilasi*
*Dr. Dario Spigolon*
*Lorenzo and my family for their precious support and their sacrifices that allowed me to do this experience*
*My "American friends", particularly Kara Barber and all my colleagues from both NGP and dual Unipa-UTMB Ph.D. Program.*

# *Introduction*

## A. Alzheimer's Disease.

### I. Alzheimer's disease pathology: An overview

Alzheimer's disease (AD) is a devastating neurodegenerative disorder leading to dementia discovered in early 900'. In fact, the clinical evaluation of an "unusual case of psychiatric illness" described by Dr. Alois Alzheimer, was reported for the first time in 1906, and this case-report gave the basis for centuries of research aiming to elucidate mechanisms causing the disease and approaches for discovering effective cures [1].

Dr. Alois Alzheimer and Dr. Gateano Perusini gave a pivotal contribute to the first histological characterization of the disease, with the drawings of *post mortem* lesions observed in their patient, in an era where the electron microscopy was not invented yet. Particularly, they found that hallmarks of the disease were neurofibrillary tangles and amyloid plaques. However, these disease hallmarks described for the first time in Alzheimer's laboratory were confirmed only 60 years later, together with the correlation between AD lesions and cognitive decline and the acceptance that AD was a common pathology of the elderly [2]. Despite the similarity of hallmarks, there are different forms of Alzheimer's disease, that can be divided into two categories that will be described in detail in the following chapter.

Histopathologically as AD progresses, it is possible to observe a massive cortex degeneration, particularly affecting the limbic regions and the subcortical nuclei. Together with cortical degeneration, it is also possible to observe an increase of ventricles diameter and a functional alteration of limbic and para-limbic structures, an alteration of Wernicke's and Broca's area and the disruption of the parietal-frontal network, thus resulting in the manifestation of the typical symptomatology characterized by: amnesia, aphasia, agnosia, apathy, language alteration, loss of

spatial orientation and executive dysfunction. These macroscopic alterations are combined with microscopic lesions, referred as amyloid plaques and neurofibrillary tangles, along with synaptic dysfunction. Amyloid plaques are large proteinaceous precipitates largely composed by amyloid beta peptides (Aβ), the cleavage product of the Amyloid precursor protein (APP). Neurofibrillary tangles are large intracellular aggregates formed by the accumulation of tau protein, a microtubule binding protein, due to hyper-phosphorylation of this protein, mainly in pyramidal neurons. However, neurofibrillary tangles are not an exclusive lesion of AD, as these lesions are characteristic also of other pathologies [3].

All lesions observed in *post mortem* AD brains are the result of decades long disease progression, and these lesions correlate only partially with the onset of the disease. [4-7]. Moreover, symptoms that can be diagnoses are the outcome of a very slow progression of the disease, that might take up to decades before it is possible to clearly diagnose the disease. In fact, as described in figure 1, initial biomarkers of AD start their manifestation several decades before the disease can be clearly diagnosed as a dementia. Particularly, the very first alteration linked to the disease is the accumulation of amyloid beta in the cerebral spinal fluid (CSF Aβ42, black cure, figure 1) during a pre-symptomatic stage of the disease and therefore almost impossible to diagnose. Subsequently, it is possible to detect other biomarkers of the disease, like amyloid deposition and hyper-phosphorylated tau protein.

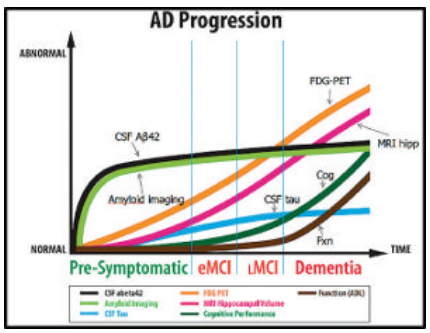


*Figure 1. AD progression and biomarkers onset. [8].*

Based on the "DSM-IV Criteria" used in clinics to assess psychiatric disorders, to be classified as "Alzheimer's disease" there should be a clear impairment of short term memory and at least one of the following symptoms: aphasia, apraxia, agnosia, executive dysfunction, and these lesions are not related to any other medical condition. Additionally, it is also taken into consideration the possible presence of one of the genetic mutations known to correlate with the disease (APP, PSEN1, PSEN2 are the genes involved) [9].

One important characteristic of AD pathology is the degree of complexity characterizing both the onset of the disease and its progression. Moreover, the increased knowledge of some of the biomolecular mechanisms leading to AD pathology, led to several controversies and to the reevaluation of several aspects of the disease. Noteworthy, the discovery of a cohort of individuals: "Non-Demented with Alzheimer's Neuropathology" (NDAN). In fact, these individuals, even though they are histopathological undistinguishable from AD patients, due to the presence of amyloid plaques and neurofibrillary tangles, their cognitive abilities are completely different, based on the cognitive tests administrated to both groups. One possible explanation to this phenomenon is that, even though levels in $A\beta_{1-42}$ are increased in both groups, the binding of Aβ to post synaptic termini in NDAN is dramatically decreased compared to AD individuals, and therefore NDAN are cognitively intact. [10-15]. This important discovery suggests that there are certain mechanisms of resistance that protects against the biomolecular alterations responsible for the disease and that effectively protects NDAN individuals against AD pathology. Hence, this evidence supports the complexity of AD pathology, and suggests the existence of complex pathways governing the progression of the disease [10, 16]. However, despite decades of research, there are no effective therapies available for reversing AD symptoms [17,18]. Possible reasons for the absence of "disease modifying therapies" are the complexity of factors leading to the onset of the disease, and the high comorbidity with other disorders [19]. Among all factors causing the disease, one of the earliest

hallmarks of AD pathology is amyloid beta peptide (Aβ) formation from amyloid precursor protein (APP) cleavage, a cascade operated by beta and gamma secretases [7, 20, 21]. As will be described in detail in a dedicated section, upon APP cleavage, Aβ is released and aggregates into toxic oligomers responsible for triggering AD pathogenesis. Nevertheless, the etiology of AD is far more complex and it cannot be excluded that the onset of the disease is triggered by a highly complex network of several factors, including aging, the impairment of protein quality control machinery and oxidative stress [22,23]. In fact, factors such as mitochondrial dysfunction, oxidative stress, dysfunction of tau phosphorylation are not unique for AD. An intriguing hypothesis is that Aβ is responsible for a chain reaction that triggers aberrant protein aggregation and overloads and impairs the "protein quality control machinery", which is already normally impaired as age progresses. Therefore, this phenomenon leads to neuronal dysfunction and loss of function. Furthermore, it is also important to consider that AD is also characterized by a high comorbidity with other diseases that are commonly present during aging, such as diabetes, hypertension, sleep deprivation and others [24-26].

Consequently, understanding how to target biological cascades responsible for AD onset is crucial to design successful therapies, that will contribute to reduce the dramatic impact of Alzheimer's disease on the society. In fact, due to the increase in elderly population, and the dramatic increase in people affected by AD that today cannot be cured, there is a prevalence of AD cases close to 40 million people worldwide [27]. Furthermore, the number of new cases is expected to increase by 2-fold every year and 16 million people affected by 2050 is the projection only in USA country [28]. Therefore, it is crucial to characterize biological cascades leading to the design of successful disease-modifying therapy.

## *II. Classification of Alzheimer's disease pathologies*

AD pathologies can be classified in two main groups: familiar and sporadic AD. Familiar AD (fAD) is mainly caused by genetic factors. fAD characterizes only 5 % of all forms of AD and, interestingly, all mutations causing the disease involve either the gene encoding for the Amyloid precursor protein (APP) or genes encoding for enzymes involved in the APP processing [29-32]. Genetic mutations either involve genes for APP, presenilin1 and presenilin 2. Furthermore, fAD can be induced by an overexpression of APP and not only by mutations; trisomy 21 is one example. This evidence suggests a pivotal role of this cascade in the pathogenesis of AD pathology [27, 33-36].

Differently from familiar AD, factors responsible for sporadic AD (sAD) are complex and heterogeneous. Moreover, the only genetic risk factor involves the ApoE ε4 variant, which either leads to an alteration of encoded isoforms of the protein or to changes in epigenetic regulation of other genes, it is only responsible for an increased predisposition to contract the sAD, [37]. Only recently, genome-wide association analysis revealed the presence of at least 20 different genes, whose alteration might contribute to sAD, but with a very low impact in the risk to develop the disease. What seems to be the main reliable contribute to the onset of sAD is aging. Furthermore, if any, the inheritance is not mendelian, even though it might occur in about 60-70% of the cases. In addition, it has been observed DNA methylation as an early event in the AD pathogenesis as another possible factor contributing to the disease onset [29]. Furthermore, increasing literature supports the hypothesis that the accumulation of Aβ is dramatically increased because of the critical impairment of clearance mechanisms [38].

## *III. The role of Amyloid β peptide in AD pathology*

On a biochemical level, AD has been defined as a "misfolding disease" [39, 40]. In fact, the main lesions characterized originally by Alzheimer in 1905, amyloid plaques and neurofibrillary tangles, are the product of misfolding and aggregation of the two most abundant proteins responsible for the onset of the disease: Amyloid β peptide (Aβ) and hyperphosphorylated tau protein. Particularly, these proteins from a naïve conformation assume an "aggregation-prone" conformation that triggers an aggregation cascade and precipitation. Based on the evidence that familial AD can be caused either by APP overexpression or mutation of either processing sites in APP, or by mutations of genes encoding for some of the cleaving enzymes involved in APP processing, it has been proposed the high contribute to the disease of the amyloid cascade [27]. However, it is important to consider that the amyloid cascade is not the only driving mechanism leading to the disease and it is not the unique cause of the disease.

Aβ peptides are 36 to 43 a. a. long peptides that are produced by the cleavage of the Amyloid precursor protein (APP), a ubiquitous type-I oriented transmembrane protein constituted by 695 residues [41]. In detail, Aβ peptides are released because of two subsequent cleavages of APP protein, operated by β- and γ-secretases This mechanism of processing is referred as "pro-amyloidogenic pathway". In fact, APP protein can be processed by two different cascades: "non-amyloidogenic" and "pro-amyloidogenic", summarized by the schematic in figure 2. Noteworthy, only the latter cascade is responsible for Aβ release from the precursor APP.

The non-amyloidogenic processing of APP is characterized by a cascade that does not produce Aβ peptides, as the cleavage of APP by α-secretase is in the middle of the sequence that releases Aβ, as summarized in the left panel of figure 2. Particularly, the first cleavage by α-secretase

generates C83 fragment that is further processed by γ-secretase into p3 fragment that is not able to aggregate and not toxic.

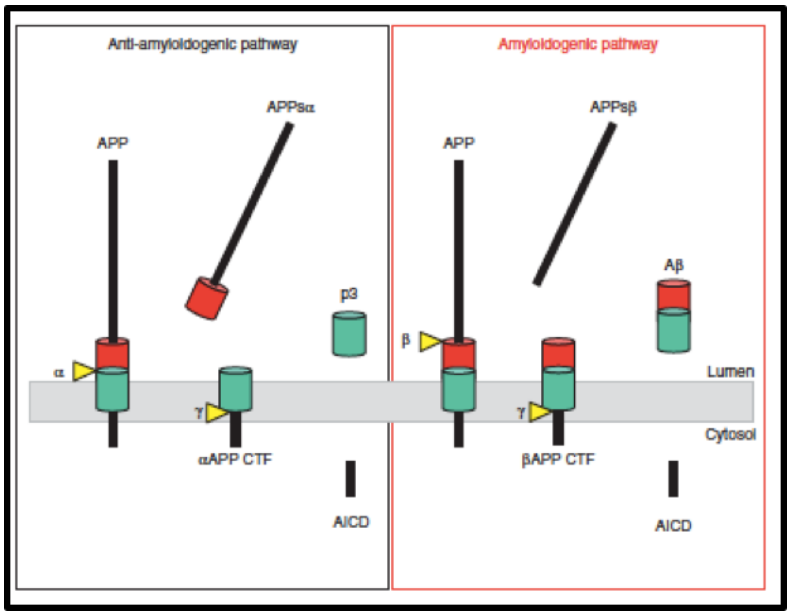


*Figure 2. Schematic representation of the two main cleavage pathways of APP protein: non-amyloidogenic (let panel) and amyloidogenic (right panel) [42].*

Conversely, as shown in the right panel of figure 2, in the pro-amyloidogenic pathway APP is first cleaved by β-secretase (BACE1) into C99 fragments and releases Aβ peptide after γ-secretase cleavage in the extracellular environment [42; 43]. The cascade leading to an increased Aβ production can be further facilitated by an alteration of the balance between amyloid production and amyloid clearance, leading to the accumulation of neurotoxic species [44].

The amyloid β peptide that is released by the pro-amyloidogenic pathway is characterized by an amorphous structure that makes the peptide prone to aggregate. The most abundant forms of human Aβ are $A\beta_{1\text{-}40}$ and $A\beta_{1\text{-}42}$. Particularly, $A\beta_{1\text{-}42}$ is the most aggressive form for its pro-amyloidogenic propensity given by the two amino acids isoleucine and alanine at the c-terminus [44, 45]. Particularly, the aggregation kinetic is characterized by a slow nucleation where small oligomers are formed (seeds), a step being the rate limiting of the whole reaction, and a fast

elongation, leading to the formation of well-organized fibers, due to the fast interaction of multiple Aβ monomers with the growing seed [46]. Figure 3 summarizes the steps of Aβ aggregation from a monomeric to a mature fibril structure.

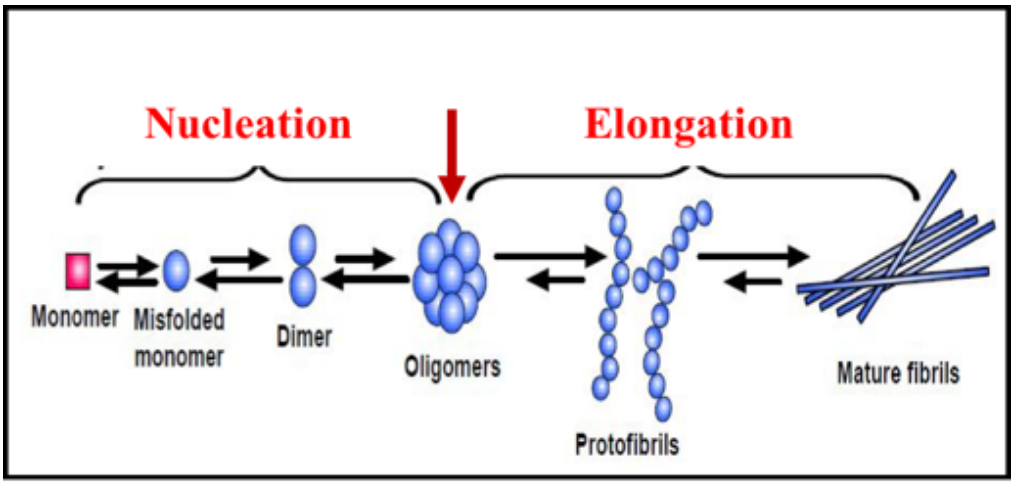


*Figure 3. Schematic representation of aggregation kinetic Aβ peptide. Monomeric Aβ, once misfolded, initiates a nucleation phase, leading to the formation of toxic oligomers indicated by the red arrow. Oligomers further aggregate into protofibrils and mature fibrils during the elongation phase. Adapted from Kumar S. and Walter J., 2011 [47].*

However, Aβ aggregation of is far more complex than the cascade described in figure 3. In fact, the amorphic structure of Aβ, due to a high abundance of intrinsically disordered regions, triggers several alternative pathways and leads to the formation of conformational different oligomers and aggregates [48, 49]. Despite all steps leading to the formation of amyloid structures, Alzheimer's disease pathology correlates mainly with oligomeric intermediated of Aβ, as demonstrated *in vitro* and *in vivo* [50-54]. Furthermore, it has been shown that oligomer toxicity is driven by their common conformation, even though the primary structure characterizing these oligomers might be of different peptides [55]. Additionally, it has also been observed the highest correlation between the pathogenesis of several neurodegenerative diseases and release of oligomers, thus suggesting the pivotal role of oligomeric structures for the onset of these diseases [56, 57].

However, despite decades of research trying to understand what triggers Aβ cascade, and how to block Aβ-induced toxicity, research has been unsuccessful so far. One of the possible explanations could be related to the instability of oligomeric forms released during the aggregation kinetic, thus making so far impossible to design effective approaches against these forms. Therefore, it is crucial to design novel approaches that can effectively target this cascade.

## *IV. AD pathology: Beyond amyloid β peptide neurotoxicity*

The main hallmark of AD is protein misfolding, thus to be considered a like "prion-like" disease, even though AD is not characterized by infectious features, differently from prion diseases [58]. Even though it seems highly established the early contribute of Aβ cascade to the onset of AD, recent studies suggest that Aβ triggers the disease but does not accelerate the progression and is not the only factor responsible for the onset of neurodegeneration [22]. Moreover, it is important to mention that also mitochondria dysfunction and alteration of glucose metabolisms have been observed in both fAD and sAD very early during the progression of the disease. Particularly, it has been observed a positive link between ApoEε4 gene variant and alteration in glucose metabolism in AD and an increase of oxidative stress leading to cytochrome C release from mitochondria. Moreover, another evidence, suggesting the role of mitochondria alterations in AD, is the increased alteration in mitochondrial DNA leading to reactive oxygen species (ROS) accumulation [59]. Furthermore, it has also been observed a high accumulation of Aβ in mitochondria, thus resulting into the alteration of electron transport chain and therefore alteration of metabolism. Indeed, the latter finding suggests a strong link between Aβ toxicity and mitochondria dysfunction [60, 61].

Another aspect involved in AD pathogenesis is tau pathology. In fact, even though tau hyper-phosphorylation and oligomerization is not unique to AD, this alteration best correlates with

synaptic dysfunction and memory loss observed in AD brains. [62] Tau protein is the most abundant microtubule-associated protein and has the physiological role in stabilizing microtubules of axons [63]. As tau protein is altered by aberrant phosphorylation, subsequent tau misfolding and oligomerization is responsible for the spreading of these toxic species and neuronal loss [6].

Overall, these considerations strongly support the concept that AD is triggered by a complex network of factors that together constitute a complex circuitry leading of the manifestation of AD pathology. A schematic representation of the possible pathways involved in AD onset and how risk factors might induce amyloid formation, tau propagation and neurodegeneration is summarized in figure 4.

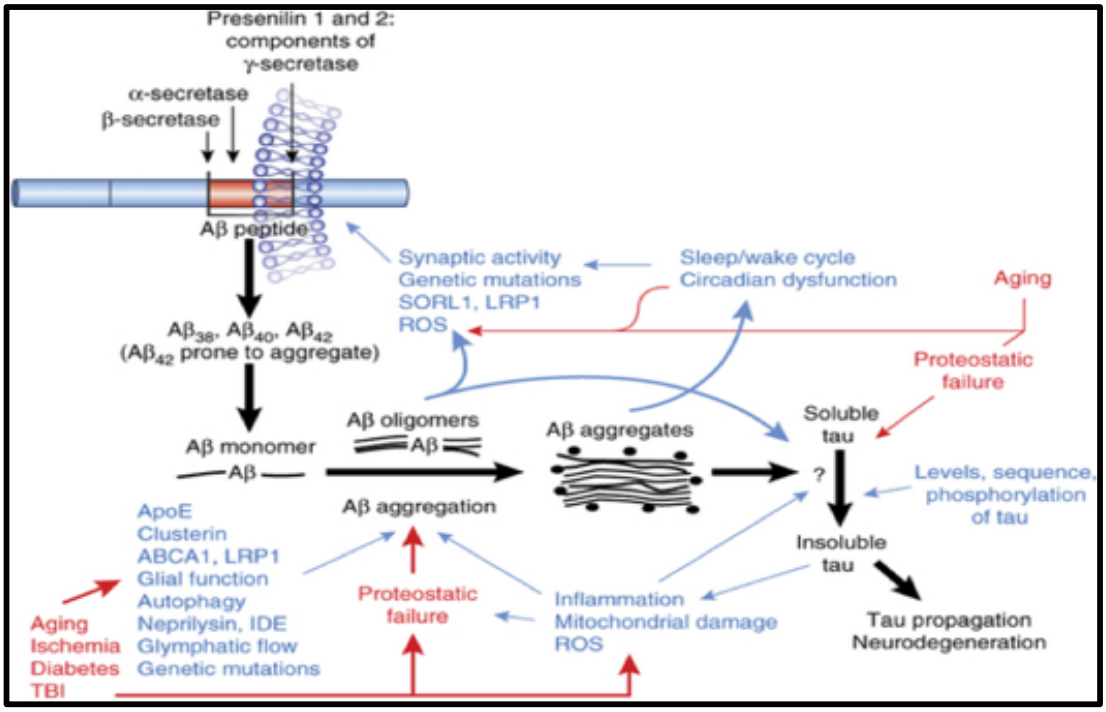


*Figure 4. Schematic representation of the complex cascade leading to neurodegeneration in Alzheimer's disease [22].*

## *V. Alzheimer's disease: Risk factors*

Depending on the form of Alzheimer's disease, there are several risk factors that contribute to the AD onset. In fact, the "early onset" form of AD is mainly triggered by genetic factors, whereas the "late onset" form of AD has only one genetic risk factor that might contribute to a predisposition to contract the disease, and an incredibly long list of risk factors that are either biological, social or environmental. To know how risk factors are linked to the onset of the disease is important, as it allows to know in advance if there is a predisposition to the disease [64]. In detail, risk factors responsible for familiar AD (fAD) are mainly genetic and are mainly mutations involving APP or enzymes involved in the processing of APP (presenilin 1 or 2, BACE 1, BACE2 and nicastrin genes), or trisomy 21 However, fAD is responsible for a low percentage of AD cases, only 2%. [65]. Conversely, the most common form of AD, sporadic AD or sAD, can be facilitated genetically only by the presence of ApoEε4 gene variant and it is mainly influenced by environmental or biological factors. Example of non-genetic risk factors are: late age, cardiovascular disorders, type II diabetes, traumatic brain injury and more [64, 66]. Particularly, aging has a pivotal role in the pathogenesis in the most common for AD. In fact, during aging there are several biochemical changes, as oxidative stress, increased inflammation, mitochondrial dysfunction, impairment of the ubiquitin-proteasome system and chaperone machinery, thus facilitating the causative factor of AD: protein misfolding [67, 68]. Unfortunately, the mechanism responsible for triggering AD onset during aging in not fully understood, as these alterations that occur during aging have a high comorbidity with other diseases [69].

## *VI. Therapeutic approaches*

AD is a known pathology for more than a century, however, all current therapies are not able to successfully cure this disease. In fact, the available therapies in the market only target certain phenotypes of the disease, but none of these approaches is a "disease-modifying" therapy. Currently, there are only two classes of FDA approved drugs, and few more compounds are only suggested adjuvants. One class of approved compounds is cholinesterase inhibitors (donepezil, galantamine and rivastigmine). The mechanism of action of these compounds is to increase acetylcholine levels through inhibiting cholinesterase action, an enzyme responsible for the degradation of the neurotransmitter and, therefore, potentiating this neuronal transmission. The use of this class of drugs is recommended mainly at initial stages of the disease, but it is also used in cases with moderate to severe AD either alone at higher doses or in combination with other drugs [70]. The mechanism of inhibition is either reversible (donepezil and galantamine) or pseudo-irreversible (rivastigmine). The other FDA approved drug is a NMDA inhibitor, memantine, which is recommended for those cases with moderate to advanced pathology. The mechanism of action of this compounds involves the glutamatergic neurotransmission, and particularly binds NMDA receptor at the Mg2+ binding site, thus preventing an aberrant activation of the receptor by glutamate. However, the beneficial effect of this treatment for AD is not clear if is because of a symptomatic effect or because of the reduction of excitotoxicity that can be caused by a synaptic accumulation of calcium induced by an increased activity of NMDA receptors in the glutamatergic synapses [71]. The use of other drugs as adjuvants, i.e. COX inhibitors or vitamins (Vitamin E or Ascorbic acid), has been suggested to protect against the increase in neuro-inflammation that has been observed during AD. Unfortunately, AD is a multi-factorial disorder with an incredibly high level of comorbidity with other disorders, thus reflecting in a constant failure of any therapeutic approach tested. In fact, genic therapy seems to be an attractive perspective [4, 71].

AD is characterized by a very slow progression; therefore, an attractive strategy could be secondary prevention. The increased interest in designing specific antibodies or probes able to bind either amyloid beta or tau protein, seems a very promising pathway toward an early diagnosis of the disease. Some examples of recent trials activated aim to test the action of antibodies against Aβ, particularly, solanezumab, gantenerumab and crenezumab. Moreover, other trials aimed to target enzymes involved in APP processing (γ-secretase and BACE1). However, all trials so far failed either in phase II or phase III [72]. Therefore, there is an urgent need for effective therapies for AD as there are none available.

# B. Chaperones: Relevance to aging and neurodegenerative disorders

## *I. Definition & Classification of Chaperones*

Chaperones are a class of ubiquitous proteins, that are highly conserved throughout evolution, and they are crucial for assisting the correct assembly of other newly synthesized proteins [73]. Moreover, these proteins are involved in the maintenance of protein and cell homeostasis throughout evolution [74]. Chaperones can be classified using several approaches. One example of classification is by molecular weight (MW) and this classification is summarized in table 1 [75]. Considering this specific classification, chaperones can be divided into: super-heavy (MW higher than 200 KDa), heavy (MW between 100-199 KDa), Hsp90s (MW between 81-99 KDa), Chaperones (MW between 65-80 KDa), Chaperonins (MW between 55-64 KDa), Hsp40 (MW between 35-54 KDa), small Hsps (MW less than 34 KDa) and other (various MW).

**Table 1. Subpopulations of Hsp chaperones[a]**

| Name | Other name(s) and/or example(s) | Mass (kDa) |
|---|---|---|
| Superheavy | Sacsin | ≥200 |
| Heavy | High MW, Hsp100 | 100–199 |
| Hsp90 | HSP86, HSP89A, HSP90A, HSP90N, HSPC1, HSPCA, LAP2, FLJ31884 | 81–99 |
| Hsp70 | Chaperones, DnaK | 65–80 |
| Hsp60 | Chaperonins (groups I and II), Cpn60 and CCT | 55–64 |
| Hsp40 | DnaJ | 35–54 |
| Small Hsp | sHsp, alpha-crystallins, Hsp10 | ≤34 |
| Other | Proteases, isomerases, AAA+ proteins (*e.g.*, paraplegin or SPG7, spastin or SPG4); α-hemoglobin-stabilizing protein | Various |

*Figure 5. Classification of chaperones by molecular weight [75].*

Attention is given to the class of "chaperonins", as part of this thesis focuses on a chaperonin belonging to this sub-class: Heat shock protein 60 or Hsp60. Overall, this class of chaperones functions once organized into a "basket-like" oligomeric structure of 7-9 units. This structure allows to assist the folding of other proteins by offering a suitable and insulated environment for proper folding of native proteins, even though chaperones never take part into the final structure of assisted proteins. Therefore, chaperonins play a pivotal role in assisting other proteins even though they do not take part in the final structure of the protein itself [76, 77]. The mechanism of this class of chaperons, characterized by interaction with the substrate, internalization, refolding and release is usually ATP-dependent and will be describe more in detail in the following chapter.

As chaperonins are a large group of chaperones with different properties, this class is further divided into two sub-classes: group I and group II. Group I chaperonins includes bacterial GroEL and eukaryotic Hsp60; group II chaperonins are thermosome expressed in Archaea or CCT and TRiC chaperonins found in cytosol of eukaryotes [78].

## *II. Structure-Activity Relationship of Chaperonins*

Chaperonins have a pivotal function in preventing protein aggregation though the assistance of the correct protein folding [79, 80]. The general mechanism is though the ability of offering a hydrophobic chamber in which a substrate can access to and refold faster and in absence of crowded environment of cytosolic compartment. Furthermore, it has been also observed that chaperonins can interact with proteins that are larger than the "folding cavity" and prevent their aggregation, thus suggesting alternative mechanisms of action [81]. Indeed, chaperones' ability to interact with their substrate thanks to the presence of "intrinsically disordered regions" (IDRs) [82]. These regions are characterized by extended molecular configuration, poor or absent secondary structure and absence of a defined tertiary structure and therefore are characterized by high flexibility [83-

85]. Indeed, these regions are the active site of the chaperone that allow the interaction with their substrate and allow the mechanism of action that is characterized by the recognition of the substrate, the assembly and the ability of modify the structure of other proteins [86].

The general structure of class I chaperonins can be summarized using GroEL as a model. In detail, the oligomer-forming unit has a secondary structure that is characterized by three main domains: apical, intermediate and e equatorial domains. The apical domain is essential for the formation of the pore to the folding cavity; the intermediate domain contributes to the overall flexibility of the structure and provides a connecting bridge between the other two domains; the equatorial domain is involved in interactions both within and between rings [87]. To be active, class I chaperonins are organized in a double ring complex, which is constituted by the assembly of two homo-heptameric oligomers. This three-dimensional conformation allows the formation of an inner hydrophobic cavity large about 45 Å, defined as the "folding chamber". Moreover, this cavity becomes even larger when the chaperone is in its active state and bound to ATP and the co-chaperon GroES, which constitutes the lid of the folding chamber. [88]. The mechanism of action of the chaperone is allowed by the positive cooperativity within rings, the negative cooperativity between rings, both ATP-dependent, and a mechanism of cyclic conformational changes [78].

The mechanism of action of class I chaperonins is also described using as a model the well-studied GroEL-GroES cycle. Particularly, GroEL assembles in a double-ring tetradecameric oligomer interacts with GroES or its substrates on the apical domain [89]. Indeed, the proper folding of substrate occurs because of a series of conformational changes of the chaperone complex. As summarized in figure 6, GroEL facilitates the proper folding of the substrate once assembled in an oligomeric complex and bound to 7 ATP molecules at the equatorial domain and GroES at the apical domain. In fact, after the formation of this complex the substrate can enter into the chaperone cavity, which is enlarged by conformational changes of the heteromeric complex. The release of

the newly folded substrate occurs upon ATP hydrolysis and ADP release. Overall, this mechanism has been referred to the model of an "Anfisen cage" [90]. ATP binding is important to trigger the cascade that leads to the complex formation with GroES and to the internalization of the protein that needs to be folded. Moreover, ATP binding is also involved in the activation of the second ring of the chaperone which triggers a new process of folding. ATP cleavage is important to facilitate the removal of GroES and the release of the newly folded protein. However, only one chamber at the time is active [91].

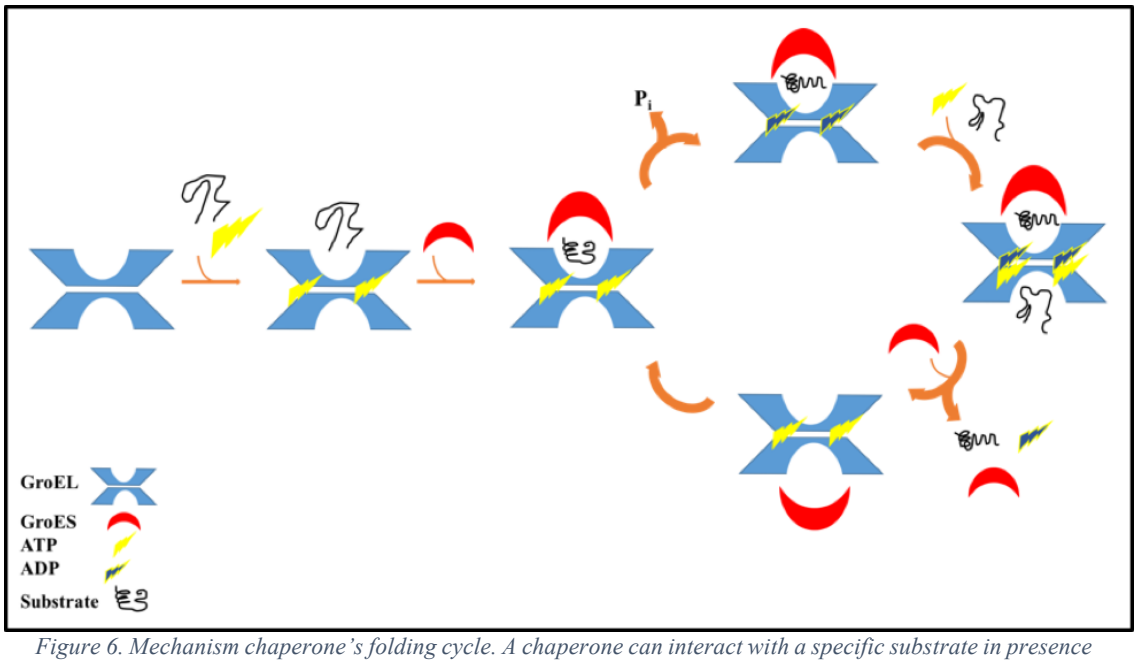


*Figure 6. Mechanism chaperone's folding cycle. A chaperone can interact with a specific substrate in presence of ATP. The refolding of the substrate occurs in the folding chamber organized by the chaperone cavity and the binding of the co-chaperone. As the substrate and ADP are released, the chaperone can start a new cycle in the second chamber. Adapted from Skjærven et al., 2015 [78].*

Human Hsp60 is a mitochondrial chaperone that is synthesized in the nucleus as a longer inactive form. Human Hsp60, despite the homology with the bacterial form, is structurally different, as it is organized by either 7 or 14 units which form either a single ring (heptameric conformation) or a double ring (tetradecamer) [92]. The 26 amino acids long sequence is referred as "leader sequence" that is important for mitochondria import. The mechanism of import of the chaperone is

highly organized and requires the presence of other chaperones in the matrix space and the correct membrane potential. The cleaved form of Hsp60 becomes active into the mitochondria via ATP-dependent process of oligomerization that is guided by other pre-existing Hsp60 oligomers [93].

The shorter and active form of Hsp60 works mainly into the mitochondria, even though action of Hsp60 has been observed also in the cytosol as pro-apoptotic mediation because of the action on the pro-caspase 3 [94].

Other functions of chaperonins are to control and minimize cellular stress due to environment stress, such as increased temperature, pH change or other stressors. Furthermore, chaperonins are also regulators of homeostatic functions, such as apoptosis, control of oxidative stress cascade, cooperate with the ubiquitin-proteasome degradation machinery [95].

Group II chaperones are characterized by higher complexity if compared to class I. In fact, despite the similar organization of oligomer-forming unit in domains, differently from group I, they from complex of 8 or 9 monomers and the oligomeric structure is mainly heteromeric, even though the interactions within and between subunits are not fully understood. Moreover, the mechanism of signaling between rings seems different between the two groups [96]. However, the mechanism of action of this group of chaperones is same as group I, as it is characterized by similar steps: formation of chaperone complex, ATP binding, interaction with the substrate in the open state, folding of the substrate in closing conformation and release of the folded substrate. However, data suggests a higher level of specialization and complexity due to the “functional polarity” of these types of chaperones. Moreover, it has been suggested a substrate-specificity for these chaperones, differently from group I [78].

## *III. Chaperones & Neurodegenerative diseases*

Chaperones are one of the most conserved guardians of cellular proteome and increasing evidence supports their important role in keeping cellular homeostasis, targeting dysfunctional proteins and facilitating the removal of toxic stressors [91, 97]. On a cellular level, proteins are exposed to crowded environments and any alteration of the balance between protective and damaging factors might induce protein dysfunction. Moreover, aging is the first factor responsible for an impairment of protective factors due to the physiological reduction of "proteostasis network" [97]. Therefore, it is not surprising that aging is the major risk factors of several pathologies characterized by protein misfolding or cancer. In fact, alterations of chaperone network have been associated with several diseases: amyotrophic lateral sclerosis, retinal degenerative disease, peripheral neuropathies and Alzheimer's disease [98]. Therefore, loss of function of chaperones have been suggested as one of the contributors in AD pathogenesis. Indeed, these proteins could be a potential target for future therapies. Noteworthy, the study showing that to potentiate the chaperone machinery in an *in vitro* model of amyloid pathology reduces Aβ-driven cytotoxicity and mitochondrial dysfunction [99]. However, there are mechanisms linking the role of chaperones and protein dysfunction observed in AD that needs further clarification, as for the presence of some controversies in the field. In fact, a gain of toxicity of certain chaperones in AD, thus resulting in an enhancement of Aβ toxicity, it has also been proposed [100]. Moreover, it has also been shown a correlation between certain proteinopathies, as polyglutamine disease, with age-related decline of the protein quality control machinery [101].

## *Aim of the dissertation*

Alzheimer's disease (AD) is the leading cause of dementia worldwide. Moreover, there is a complex etiology responsible for the onset of AD, thus making so far impossible to find effective disease-modifying therapies. There are several hypotheses suggesting possible mechanisms involved in AD onset, however, the pro-amyloidogenic cleavage of amyloid precursor protein (APP), leading to amyloid beta peptide (Aβ) formation, misfolding and subsequent neurotoxicity, seems one of the most accredited. Moreover, there is evidence suggesting that a failure of the protein quality control machinery also contributes to AD onset, thus confirming that the main risk factor of late onset AD is aging. One important component of the protein quality control machinery is the family of chaperones, particularly, the focus of my thesis in one of the most evolutionary conserved chaperone: Hsp60. This mitochondrial chaperonin is involved both in protecting mitochondria from damage induced by misfolded protein on a cellular level, and in a cross-talk with the immune system on a systemic level. Additionally, it has been shown that Hsp60 is directly involved in an interaction with APP/Aβ and in a downstream protection of mitochondria from Aβ-induced damage. Therefore, the aim of this dissertation is to determine the functional effect of Hsp60 on Aβ, either in its monomeric or oligomeric structure, and to investigate if this interaction leads to the formation of less toxic conformations. My central hypothesis is that Hsp60 effectively inhibits Aβ aggregation and toxicity. I addressed my central hypothesis with three specific aims. I first confirmed that Hsp60 has a direct effect in inhibiting the aggregation of Aβ using a cell free system. I addressed my aim using circular dichroism, Thioflavin T assay, size exclusion chromatography and atomic force microscopy. In my second specific aim, I tested the working hypothesis that to overexpress Hsp60 influences APP processing and Aβ release using an *in vitro* approach. I addressed my second aim creating a novel cellular model that overexpresses both the

amyloid precursor protein (APP) and Hsp60 and, as I validated the model by western blotting and immunocytochemistry, I investigated the effect of Hsp60 on APP and Aβ in different sub-cellular compartments: extracellular, intracellular and mitochondria. Finally, in my third aim, I confirmed that, upon Hsp60 treatment, Aβ formed less toxic oligomers, thus resulting in reduction in neuronal death *in vitro*. I addressed my third aim using a neuroblastoma cell line as an *in vitro* model, and I tested changes in cytotoxicity of either human Aβ oligomers produced *in vitro* or pre-formed oligomers, both before and after Hsp60 exposure. I parallel experiments, I investigated the levels of Hsp60 in *post mortem* tissues of Alzheimer's disease individuals, compared to healthy controls, using western blotting to confirm that during Alzheimer's disease there is an impairment of the chaperone machinery, with attention to Hsp60. As the field is controversial about the role of Hsp60 in AD, this project will contribute to elucidate crucial mechanisms of action of Hsp60, thus proposing this chaperone as a potential target for future therapies against AD pathology.

# *Experimental approach*

## I. Material and Methods

-Amyloid β peptides*:* $A\beta_{1\text{-}40}$ (Anaspec) preparation for biophysical analysis is using a standardized protocol published by Fezoui et al. [102]. In detail, the peptide was solubilized in NaOH 5 mM (pH 10) and aliquots deeply frozen in liquid nitrogen, lyophilized and stored at -80 °C upon use. Before each experiment, lyophilized aliquots were solubilized in Tris HCl 20 mM (pH 7.7), and filtered using to filtered installed in series with 0.20 μm (Whatman) and 0.02 μm (Millex-Lg) respectively, to remove larger aggregates or impurities. All procedures were done in a cold room kept at 4 °C. The initial concentration of the sample was determined spectrophotometrically per Lambert-Beer equation using tyrosine absorption at 276 nm and a molar extinction coefficient of 1390 $cm^{-1}$ $M^{-1}$ [103]. All aggregation kinetics were performed at controlled temperature (37 °C) and agitation (200 rpm) for a total time of 24 hours. Aliquots of $A\beta_{1\text{-}40}$ used for SEC-HPLC injections were concentrated after chromatographic elution with 3 KDa cut-off filters (Millipore) by centrifugation at 6000g and 5 °C, using a centrifuge Heraeus Multifuge X3R. Samples of $A\beta_{1\text{-}40}$ 50 uM for AFM measurements, either treated or not with Hsp60 2uM, were adsorbed on MICA surface either at time 0 or after 3 days of the aggregation kinetic. $A\beta_{1\text{-}42}$ *monomers*, for experiments of aggregation kinetics in cell free system, were produced from a recombinant peptide produced and purified as previously described [104]. Frozen lyophilized fractions were then prepared using the same protocol used for $A\beta_{1\text{-}40}$ as previously described. The aggregation kinetic was performed either using a final concentration of 50 μM or 15 μM. The concentration chosen to test the effect of Hsp60 was 15 μM, due to the high aggregation rate of this peptide.

*Aβ oligomers* for *in vitro* experiments per prepared as previously published [53]. Briefly, 1 mg of lyophilized peptide is solubilized in 1.5 ml acetonitrile/water 1:1 (v/v), to remove impurities.

The suspension is left room temperature for 10-15 minutes and aliquoted into three 1 ml tubes (Eppendorf) and further lyophilized and stored at -20 °C upon use. The day of the experiment aliquots are suspended in Hexafluoro-2-propanol, HFIP (200 μL for each aliquot used) and left at room temperature for 10-20 minutes. The solution is then transferred in a new tube with a stirrer and diluted with DDI water (700 μL for each aliquot), gently mixed and covered with a cap with holes. The peptide is left oligomerize at room temperature and under agitation for 2 days. Oligomers are either used immediately or stored at -80 °C until use. The quality of Aβ oligomers is confirmed by dot blot assay using either 6E10 (mouse, Covange) antibody or A11 (rabbit, Covance).

-*Hsp60*: for biophysics experiments, human variant of mitochondrial Hsp60 (short form, ATGen), was subjected to buffer change from 20 mM Tris HCl (pH 8), 100 mM NaCl, 10% Glycerol to the desired final buffer using centrifuge filtering devices with a 30 KDa cut-off (Amicon Ultra 4, Millipore). Final conditions were the following: 20 mM Tris HCl (pH 7.7), 30 mM NaCl, 3% Glycerol. Prior to each experiment, protein stability was estimated using light scattering technique. For cell culture experiments, aliquots of Hsp60 were diluted up to 2 μM or 1 μM in buffer PBS 1X and further diluted in DMEM/F12 up to 10 times for cytotoxicity experiments. All sample preparation procedures were conducted in asepsis. All samples' final concentrations were calculated mathematically and final samples prepared either in cold room or in ice.

-Thioflavin T Assay. Thioflavin T (ThT) is a benzothiazolic compound used to detect amyloid aggregation for the ability to fluoresce in presence of β-sheet rich structures, as the two aromatic rings of its chemical structure becomes more conjugated in presence of fibers and therefore contributes to an increase in intensity of emission [105]. All experiments are performed using ThT 12 μM added to sample aliquots and emission spectra recorded with a JASCO FP-6500 spectrophotometer. In all experiments excitation wavelength was 450 nm and kinetic of emission

was acquired at 485 nm. Slit width was fixed at 3 nm. All samples were incubated at 37 °C and stirred at 200 rpm [106].

-Circular Dichroism (CD) spectroscopy. The use of this spectroscopic technique allows to characterize the secondary structure and the three-dimensionality of proteins, due to the asymmetrical structure and therefore its different ability to interfere with circularly polarized light [107]. All CD spectra are measured using a JASCO J-815 CD spectrometer on a small aliquot of sample (50 μL) loaded on a 0.2 mm path length quartz cuvette. All recordings were done at 20 °C and each spectrum showed in the results section is the average of 8 scans and the result of solvent subtraction [106].

-Atomic Force Microscopy. Morphology information of samples of either $A\beta_{1-40}$ or $A\beta_{1-40}$ exposed to Hsp60 were obtained thanks to a collaboration with the "Istituto Italiano di Tecnologie" in Genoa (IT), using a Nanowizard III (JPK Instruments, Germany) either mounted on a Axio Observer D1 (Carl Zeiss, Germany) or on an Eclips Ti (Nikon, Japan) microscopes. For each sample, small aliquots were adsorbed on a freshly cleaved mica surface (Agar Scientific, Assing) for 20 minutes, washed with deionized water and dried with pressurized nitrogen. The morphology of each sample was obtained using an "intermittent contact mode in air", using a NCHR silicon cantilever (Nanoworld). The nominal spring constant ranged between 21 and 78 N/m and the resonance frequency between 250 and 390 kHrz [106].

-HPLC. All chromatographic analyses were done using a HPLC machine (Prominence, Shimatzu) assembled with a mobile phase degasser (DGU-20As), a quaternary pump (LC-2010 AT) and 500 μL injection loop. To elute samples by size, Superdex 200 (10 300 GE Healthcare) column was used to separate samples, and as mobile phase 20 mM Tris HCl (pH 7.7), 3 % glycerol, 30 mM NaCl. Flow rate for samples elution was controlled at 0.5 $mL/min^{-1}$. Samples detection was done using a photodiode array detector (SPD-M20A) and chromatograms recorded at 280 nm [106].

-Cell culture. Chinese Hamster Ovary cells (CHO) and 7PA2 cell line, CHO overexpressing human APP variant with the Swedish mutation were generously donated by Dr. Dennis Selkoe at Harvard Medical School, Boston, MA, kindly donated from Selkoe DJ at Harvard, USA) were kept in culture for less than 10 passages with DMEM (Corning), 10% FBS (heat inactivated 15 minute, 56 °C, Sigma Aldrich), 1% penicillin/streptomycin (Gibco), without (CHO cells) or with G418 (7PA2 cells, Gibco). 7PA2/H60 cell line was kept in culture for less than 10 passages with DMEM (Corning), 10% FBS (heat inactivated 15 minute, 56 °C, Sigma Aldrich), 1% penicillin/streptomycin (Gibco), G418 0.6 mg/mL and Hygromicin B (Corning) 0.6 mg/ml. SH-SY5Y neuroblastoma cell line was grown in DMEM/F12 (Corning), 10% FBS (heat inactivated 15 minute, 56 °C, Sigma Aldrich), 1% penicillin/streptomycin (Gibco) and cells were seeded on a 24- or 96-wells plates, the day before each treatment in regular media end treatments were given in DMEM/F12 for 24 hours.

-Sub-cellular fractionation: Mitochondria were isolated using a preparation kit [Qproteome, Mitochondria isolation kit, Qiagen] and the quality of the preparation validated by western blotting; extracellular environment was isolated using a protocol optimized for obtaining a media enriched in Aβ, referred as "conditioned media" (CM) using a revised protocol published by Meli et al. [108].

-Plasmid transfection: Overexpression of plasmids, either empty pCMV6 or pCMV6-Hsp60 (both OriGene), has been done with Lipofectamine 2000 (Life technologies, Protocol Pub. No. MAN0007824 Rev.1.0) using manufacturer's recommended protocol [109]. In detail, one day prior to transfection, cells were seeded to be 70% confluent at moment of transfection. Concentrations of lipofectamine and plasmids were optimized to obtain a high transfection efficiency. Prior transfection, lipofectamine was diluted and mixtures left 10 minutes at room temperature. Subsequently cDNA at proper concentration was added to lipid complex and reaction between

reagents allowed for further 10 minutes. Transfection of cells was blocked after 5 hours with media enriched with serum and antibiotics free. After 24 hours, cells are washed and initial media replaced with antibiotics-enriched media. Efficiency of transfection was tested either 48 hours or after 1 month of transfection by western blotting and immunocytochemistry as described below.

- Cytotoxicity Assay. Cell death was measured after 24 hours' treatments using the "Cytotoxicity Assay kit" (Roche) and procedures were done using manufacturer protocol. Briefly, cytotoxicity is calculated as the function of absorbance of a dye sensitive di lactate dehydrogenase released un the culture media by damaged cells. The colorimetric reaction is then detected by a multiplate reader (μQuant, Biotek) and cytotoxicity calculated as a percentage using the following formula: Cytotoxicity (%)= [(experimental value – low control)/ (high control – low control)] *100.

Low control was calculated using media from cells treated with serum-free culture media (DMEM/F12 medium, Sigma Aldrich); high control was calculated using media from cells treated with 10% Triton-X 100 serum free culture media. All samples used for cell treatments were diluted 1:10 or 1:5 in serum-free culture media. Cells were treated either with oligomers, Hsp60, oligomers exposed to Hsp60, 7PA2 CM, CHO conditioned media (CM), 7PA2 CM or 7PA2/H60 CM.

- Western Blotting (WB). All blots were done in denaturing conditions. Electrophoretic run is performed at constant voltage (100 V for 10 minutes and 120 V until the end of the run). Protein were transferred on a nitrocellulose membrane at 0.4 A for 1 hour 30 minutes in ice or 0.02 A for 18 hours if total proteins loaded was equal to or higher than 100 μg. Antigen retrieval was then performed by microwaving the membrane in PBS buffer 1 minute and then 30 seconds after a wash of 4 minutes in fresh PBS. Proper transfer of the proteins was assessed with Ponceau Red and membranes were then blocked with Odyssey blocking solution at room temperature for 1 hour. 6E10 (1:1000, Covance) has been used to detect APP; anti-Hsp60 (1:5000, Abcam) has been used to detect the total amount of Hsp60 expressed; DDK antibody (1:1000, OriGene) has been used to

detect the recombinant protein overexpressed after plasmid transfection. Blots acquisition were performed with Odyssey LI-COR using manufacturer's protocol and quantifications were obtained with ImageJ software.

- Immunocytochemistry (ICC). All confocal images have been done on fixed cells with methanol/acetone and mounted on Super/frost slides (Fisherbrand, Fisher scientific), using a Nikon A1+ confocal microscope. Cells were seeded on coverslips 24 hours prior to immunocytochemistry and washed twice with cold PSB. Cells were then fixed and left 1 hour on ice. Cells were then washed twice for 5 minutes with cold PBS and blocked 1 hours with 3% BSA and 0.05% Tween 20 in PBS. All primary antibodies were incubated for 18 hours at 5 ºC and secondary antibodies were incubated 1 hour at room temperature away from light, after two 10 minutes' washes with PBS. In detail, nuclei are stained with DAPI, Aβ/APP is stained with 6E10 antibody (mouse, Covance), total Hsp60 is stained with anti-Hsp60 antibody (rabbit, Abcam or Origene), recombinant Hsp60 is stained with anti-DDK antibodies (mouse Origene o rabbit, Santacruz). Secondary antibodies are Alexa-594 (red, mouse or rabbit, Abcam), Alexa-488 (green, mouse or rabbit, Abcam). All antibodies were properly diluted in PBS 1.5% normal goat serum (NGS)

- ELISA. Quantitative analysis of total Aβ was done using manufacturer protocol for Human Aβ42 ELISA kit (life technologies) on culture media isolated from CHO, 7PA2 and 7PA2/H60 cell lines and prepared following a revised protocol published Meli G. et al. 2014 [108].

# II. Results

## 1. Investigating the inhibitory effect of Hsp60 on Aβ aggregation using a "cell free" model.

- *Hsp60- Aβ1-40 protein/protein interaction in a cell free system: model validation*

I first tested the hypothesis that Hsp60 successfully inhibits $A\beta_{1-40}$ aggregation. To support my hypothesis, I first characterized all optimal conditions for testing a correct protein-protein interaction in a cell free model. The rationale of this investigation lays on the principle that the physical interaction between $A\beta_{1-40}$ and Hsp60 is known in literature, as immunoprecipitation data (IP) has been previously reported [100]. However, the mechanism of interaction between these two proteins is not fully understood. Table 1 summarizes the concentrations tested of both $A\beta_{1-40}$ peptide and Hsp60, and buffer composition used to solubilize both peptides. Particularly, I tested $A\beta_{1-40}$ 50 μM and 25 μM either without or exposed to the mitochondrial form of Hsp60 (short Hsp60 or Hsp60s) at 1 μM or 2 μM concentrations. The approach I used to test the effect of Hsp60 on $A\beta_{1-40}$ aggregation is based on a well characterized protocol of amyloid β aggregation [110, 111], which allowed a controlled aggregation kinetic toward fiber formation. In summary, the aggregation kinetic was controlled for a time of at least 24 hours under constant temperature of 37 °C and agitation of 200 rpm. Each condition used is summarized in table 1 and each sample was tested using Thioflavin T assay and CD measurements of time points of the aggregation kinetic, as these were very well established assays for characterizing $A\beta_{1-40}$ aggregation kinetic. Particularly, it has been already described in material and methods that ThT is a probe whose fluorescence increased in presence of aggregates in solution, for a conformational flexibility that allowed an increased conjugation in presence of amyloid fibers. Therefore, this was a valid and reproducible technique

for the indirect measure of $A\beta_{1-40}$ aggregation kinetic. On the other hands, circular dichroism gave direct information about the folding state of the proteins analyzed, due to the specific interaction between the asymmetrical conformation of the protein and the circularly polarized light of the instrument.

*Table 1. Optimization of working conditions for testing Aβ-Hsp60 interaction*

| Conditions | 1 | 2 | 3 | 4 | 5 | 6 | 7 | 8 |
|---|---|---|---|---|---|---|---|---|
| [$A\beta_{1-40}$] | 50 µM | 50 µM | 50 µM | 50 µM | 25 µM | 50 µM | - | - |
| [Hsp60s] | - | 1 µM | - | 2 µM | - | 2 µM | 1 µM | 2 µM |
| Buffer | 20 mM Tris HCl | 20 mM Tris HCl, 1.5% glycerol, 15 mM NaCl | 20 mM Tris HCl 3% glycerol, 30 mM NaCl | 20 mM Tris HCl, 3% glycerol, 30 mM NaCl | 20 mM Tris HCl, 10% glycerol, 100 mM NaCl | 20 mM Tris HCl, 10% glycerol, 100 mM NaCl | 20 mM Tris HCl, 1.5% glycerol, 15 mM NaCl | 20 mM Tris HCl, 10% glycerol, 100 mM NaCl |
| rpm | 200 | 200 | 200 | 200 | 200 | 200 | 200 | 200 |
| pH | 7.4 | 7.4 | 7.4 | 7.4 | 7.4 | 7.4 | 7.4 | 7.4 |
| T | 37 °C | 37 °C | 37 °C | 37 °C | 37 °C | 37 °C | 37 °C | 37 °C |
| [ThT] | 12 µM | 12 µM | 12 µM | 12 µM | 12 µM | 12 µM | 12 µM | 12 µM |

However, it was important to consider that, even though the main goal of using CD technique was to characterize Aβ secondary structure, also Hsp60 had a signal in the range of wavelengths in which Aβ absorbs. In fact, figure 7 shows a kinetic of Hsp60 2 µM at different time points (0, 1, 3, and 5 hours) and it is possible to observe the intense alpha-helix signal that is stable over time and that could cover structural information given by Aβ peptide spectra. Therefore, all CD spectra of $A\beta_{1-40}$ and Hsp60 kinetics reported in the following chapter were presented subtracting the contribute Hsp60 CD spectrum.

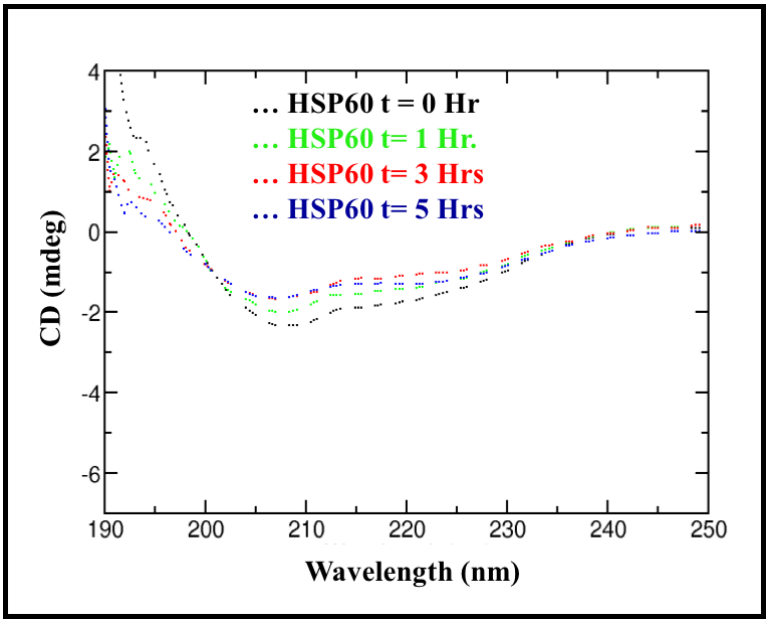


*Figure 7. CD spectra of Hsp60 2 µM at different time points of an incubation kinetic: 0 (black dotted line); 1 hour (green dotted line); 3 hours (red dotted line); 5 hours (blue dotted line). Experimental conditions: buffer 20 mM Tris (pH= 7.7), 3% glycerol, 30 mM NaCl, T = 20 °C.*

Figure 8 shows both ThT assay (panel A on the left) and CD spectra (panel B on the right) on 5 time points of the aggregation kinetic of a sample of $A\beta_{1\text{-}40}$ 50 µM in 20 mM Tris HCl buffer (pH 7.4), time 0, 1 hour, 3 hours, 5 hours and 24 hours. Consistent with the extensive literature available [112-114], time course fluorescence of ThT was characterized by an initial low signal referred as lag phase, representing the nucleation phase of Aβ seeds, followed by an exponential increase in intensity of emission until a plateau, representing the elongation phase of aggregates and the formation of amyloid fibers. In these conditions of temperature, buffer, pH and agitation, Aβ fibers were formed in about 6 hours. In fact, at time 0 of the aggregation kinetic the CD spectrum of the protein (black spectrum, figure 8) was characterized by a minimum around 195 nm, which was typical of a random coil conformation characterizing unordered and not aggregated structures. As soon as Aβ was incubated under pro-aggregating conditions, there was a change in its CD spectrum that already after 5 hours (blue spectrum) was characterized by a shift of the minimum around 210 nm, typical of β-sheet conformations of aggregated proteins. The aggregation of Aβ is even more

pronounced after 24 hours (light blue spectrum, figure 8 B), as the CD spectrum is characterized by a shape of a sigmoid with two minima in the range on 215 nm and 220 nm respectively.

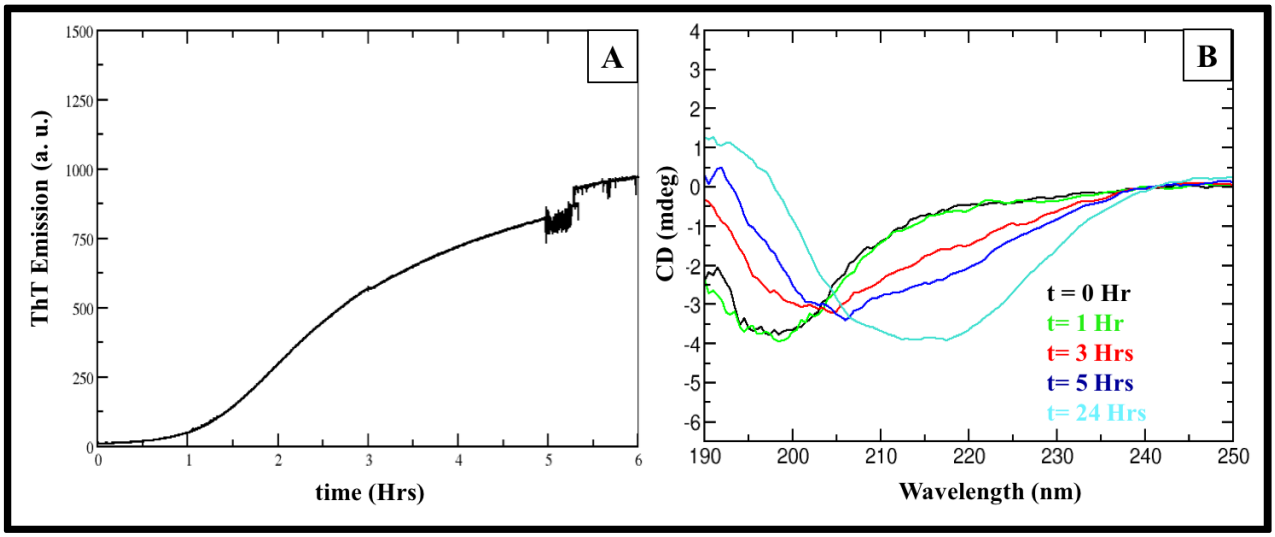


*Figure 8. Characterization of Aβ1-40 aggregation kinetic using ThT and CD assays. A. ThT assay of Aβ1-40 in 20 mM Tris HCl buffer (pH 7.7) incubated at 37 ◦ C and stirred at 200 rpm in presence of ThT. λxcThT=450 nm; λemThT=484 nm. B. CD spectra of Aβ1-40 at different time points of the aggregation kinetic: 0 (black line), 1 hour (green line), 3 hours (red line), 5 hours (blue line) and 24 hours (light blue line). Measures recorded at 20 ◦ C.*

Once defined the biophysics properties of $A\beta_{1\text{-}40}$ 50 µM in this specific experimental conditions, I tested the effect of different concentrations of Hsp60 (1 µM and 2 µM respectively) on the aggregation kinetic using the same techniques: ThT assay and CD analysis at specific time points as previously described. As summarized in figure 9, in these experimental conditions, Hsp60 1 µM influenced $A\beta_{1\text{-}40}$ aggregation kinetic, as it was possible to observe a longer lag phase with the ThT assay (panel A, figure 9), which suggested a change in the nucleation phase. In addition, CD spectra of time points of the aggregation kinetic suggested that the presence of Hsp60 inhibited Aβ aggregation when compared to $A\beta_{1\text{-}40}$ alone (panel B, figure 9). Particularly, it was possible to observe that CD spectrum at 3 hours of $A\beta_{1\text{-}40}$ treated with Hsp60 under pro-aggregating conditions (red spectrum, figure 9B) had a similar morphology of monomeric $A\beta_{1\text{-}40}$ at (black spectrum figure

9 B). On the other hands, untreated $A\beta_{1\text{-}40}$ spectrum after 3 hours (dotted spectrum in red, figure 9B) had a different morphology compared to time zero, thus suggesting aggregates formation. The difference in conformation of $A\beta_{1\text{-}40}$ treated with Hsp60 was even more pronounced if compared CD spectra at 5 hours of aggregation kinetic (blue continuous line compared to blue dotted line, figure 9B).

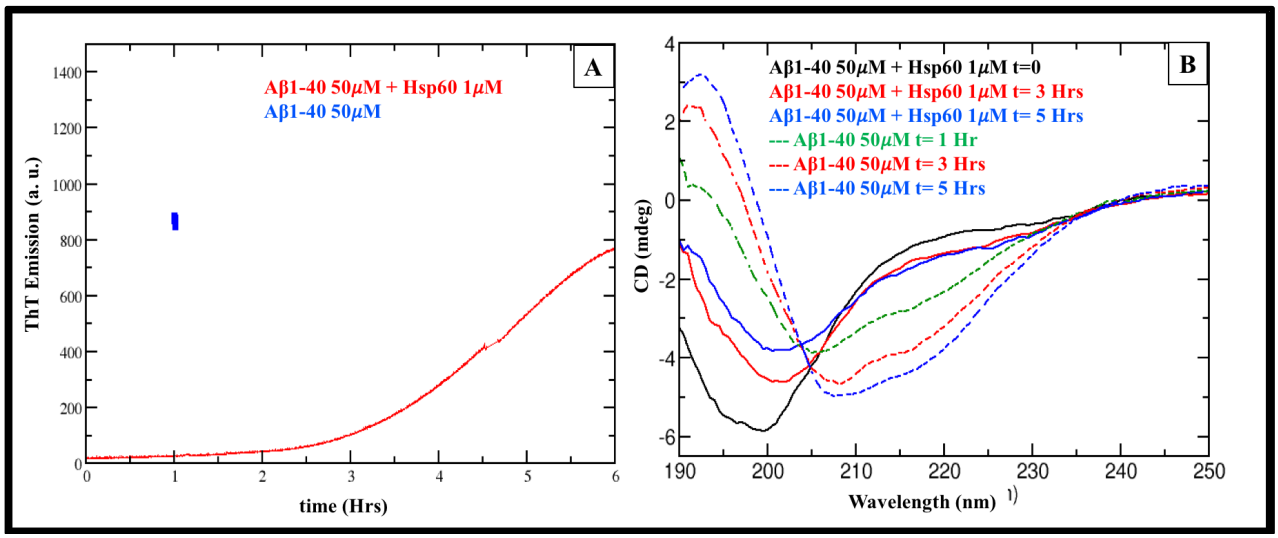


*Figure 9. Characterization of Aβ1-40 aggregation kinetic with Hsp60 1μM using ThT and CD assays. A. ThT assay suggests that the presence Hsp60 delays the aggregation kinetic (red line) compared to the control (blue time point). Both kinetics is performed in 20 mM Tris HCl buffer, 1.5 % glycerol, 15 mM NaCl (pH 7.7), T = 37 ◦C, agitation 200 rpm, ThT 12 μM. λexcThT=450 nm; λemThT=484 nm. B. CD spectra of Aβ1-40 50μM with Hsp60 1μM at different time points of the aggregation kinetic: 0 hour (black line), 1 hour (green line), 3 hours (red line), 5 hours (blue line), compared to Aβ1-40 kinetic: 1 hour (green dotted line), 3 hours (red dotted line), 5 hours (blue dotted line). Data suggests a change in Aβ conformation in presence of Hsp60, due to a delay of aggregation. Measures done at 20 ◦C.*

Moreover, I wanted to investigate if an increase of Hsp60 concentration could completely inhibit $A\beta_{1\text{-}40}$ aggregation kinetic. Therefore, a sample of $A\beta_{1\text{-}40}$ 50 μM was either exposed or not to Hsp60 2 μM in buffer 20 mM Tris HCl (pH 7.7), 10% glycerol and 100 mM NaCl (figure 10). As confirmed by ThT assay in figure 10A, Hsp60 in these conditions successfully delayed the nucleation phase of amyloid beta kinetic, even though the formation of fibers was not inhibited. However, it is known from literature that high ionic strength is a factor facilitating protein

aggregation. Therefore, I tested the same concentration of the two proteins but in milder conditions: 20 mMTris HCl pH 7.4, 3% glycerol, 30 mM NaCl. Results are shown in figure 11.

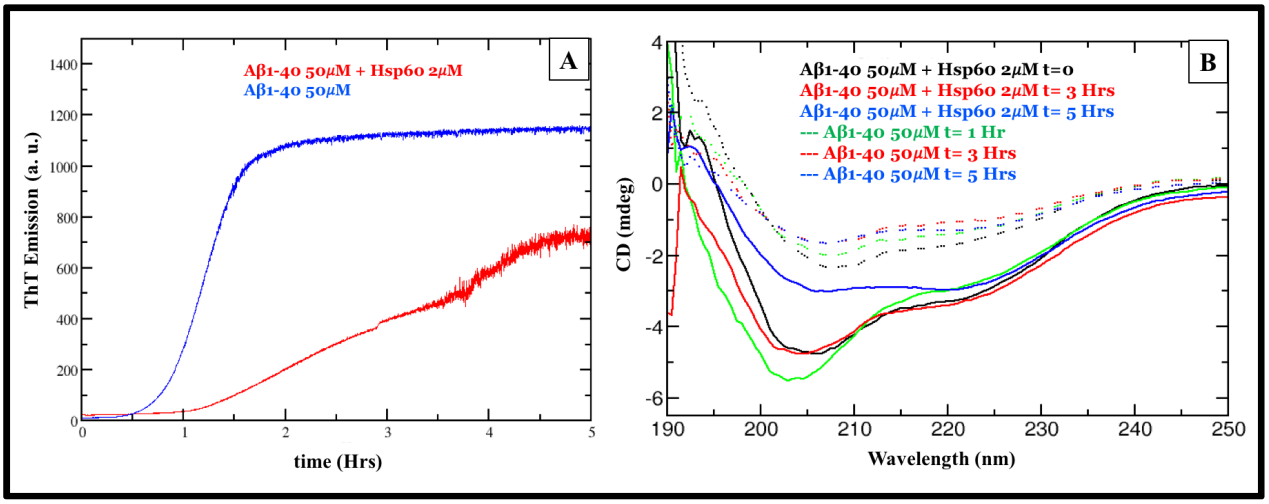


*Figure 10. Characterization of aggregation kinetic of Aβ1-40 50μM with Hsp60 2μM in high salt concentration buffer, using ThT and CD assays. A. ThT assay suggests that Hsp60 delays Aβ aggregation kinetic (red line) compared to the control (blue line). Both kinetics is performed in 20 mM Tris HCl buffer, 10 % glycerol, 100 mM NaCl (pH 7.7), T = 37 ◦C, agitation and 200 rpm, ThT 12 μM. λexcThT=450 nm; λemThT=484 nm. B. CD spectra of Aβ1-40 50μM with Hsp60 2μM at different time points of the aggregation kinetic: 0 hour (black line), 1 hour (green line), 3 hours (red line), 5 hours (blue line), compared to Aβ1-40 50μM kinetic: 0 hour (black dotted line), 1 hour (green dotted line), 3 hours (red dotted line), 5 hours (blue dotted line). Data suggests a change in Aβ conformation in presence of Hsp60, due to a delay of aggregation. Measures done at 20 ◦C.*

Interestingly, in these conditions Hsp60 had a very strong effect in blocking $A\beta_{1-40}$ aggregation kinetic. In fact, as summarized in figure 11, panel A, ThT assay of $A\beta_{1-40}$ treated with Hsp60 2 μM (red line, figure 11 A) did not form seeds able to trigger the exponential aggregation phase, as observed in the untreated $A\beta_{1-40}$ sample (blue line, figure 11 A). Therefore, this data suggested that $A\beta_{1-40}$ exposed to Hsp60 lost the ability to aggregate. This data was further confirmed by CD analysis summarized in Figure 11 panels B and C. Particularly, in figure 11 B are compared CD spectra of $A\beta_{1-40}$ either with or without Hsp60 at time zero, 1 hour, 3 hours and 5 hours. Moreover, in figure 11 C are compared CD spectra of both proteins at time zero and 24 hours. Overall, CD spectra analysis suggested that Hasp60 inhibited $A\beta_{1-40}$ aggregation, because the presence of the

chaperone changes Aβ spectrum morphology. Particularly, the phenomenon is clear when compared to the untreated peptide at the time point of 24 hours (dotted red line compared to red line in figure 11 C).

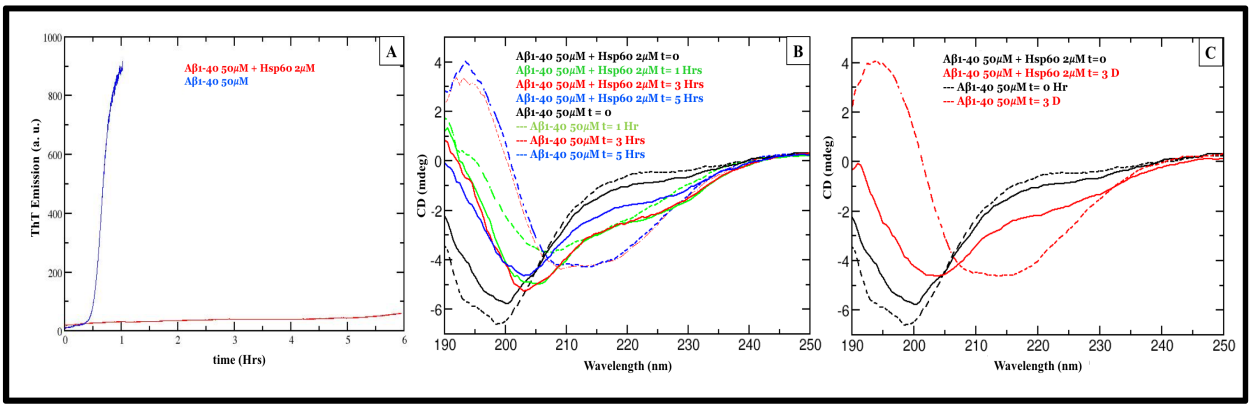


*Figure 11. Characterization of aggregation kinetic of Aβ1-40 50 μM with Hsp60 2μM using ThT and CD assays. A. ThT assay suggests Hsp60 inhibits Aβ aggregation kinetic (red line) compared to the control (blue time point). Both kinetics is performed in 20 mM Tris HCl buffer, 3 % glycerol, 30 mM NaCl (pH 7.7), T= 37 ◦C, agitation 200 rpm, agitation ThT 12 μM. $\lambda_{excThT}$=450 nm; $\lambda_{emThT}$=484 nm. B. CD spectra of Aβ1-40 50μM with Hsp60 2μM at different time points of the aggregation kinetic: 0 hour (black line), 1 hour (green line), 3 hours (red line), 5 hours (blue line), compared to Aβ1-40 50μM kinetic: 0 (black dotted line), 1 hour (green dotted line), 3 hours (red dotted line), 5 hours (blue dotted line). Data suggests a change in Aβ conformation in presence of Hsp60, due to a delay of aggregation. All CD spectra are performed at 20 ◦C. C. CD spectra of Aβ1-40 50μM with Hsp60 2μM, compared to Aβ only, at time zero (black lines) or after 3 days (red lines).*

- *Hsp60- Aβ1-40 protein/protein interaction in a cell free system: AFM morphology*

To further validate the effect of Hsp60 on $A\beta_{1-40}$ aggregation, samples of $A\beta_{1-40}$, either exposed or not Hsp60 were analyzed with atomic force microscopy (AFM) for morphologic characterization at time zero and after 24 hours of aggregation kinetic. Data summarized in figure 12 were done in collaboration with ITC in Genova by Dr. Canale. In detail, consistent with data from several other laboratories, as $A\beta_{1-40}$ is under pro-aggregating conditions for 24 hours, it formed long fibers that were in the range of microns (figure 12 panels a and b). Consistent with CD and ThT assays previously shown, the presence of Hsp60 completely inhibited the formation of $A\beta_{1-40}$ fibers, as there was no morphological difference between samples analyzed at time zero and after 24 hours of aggregation (figure 12, c and d).

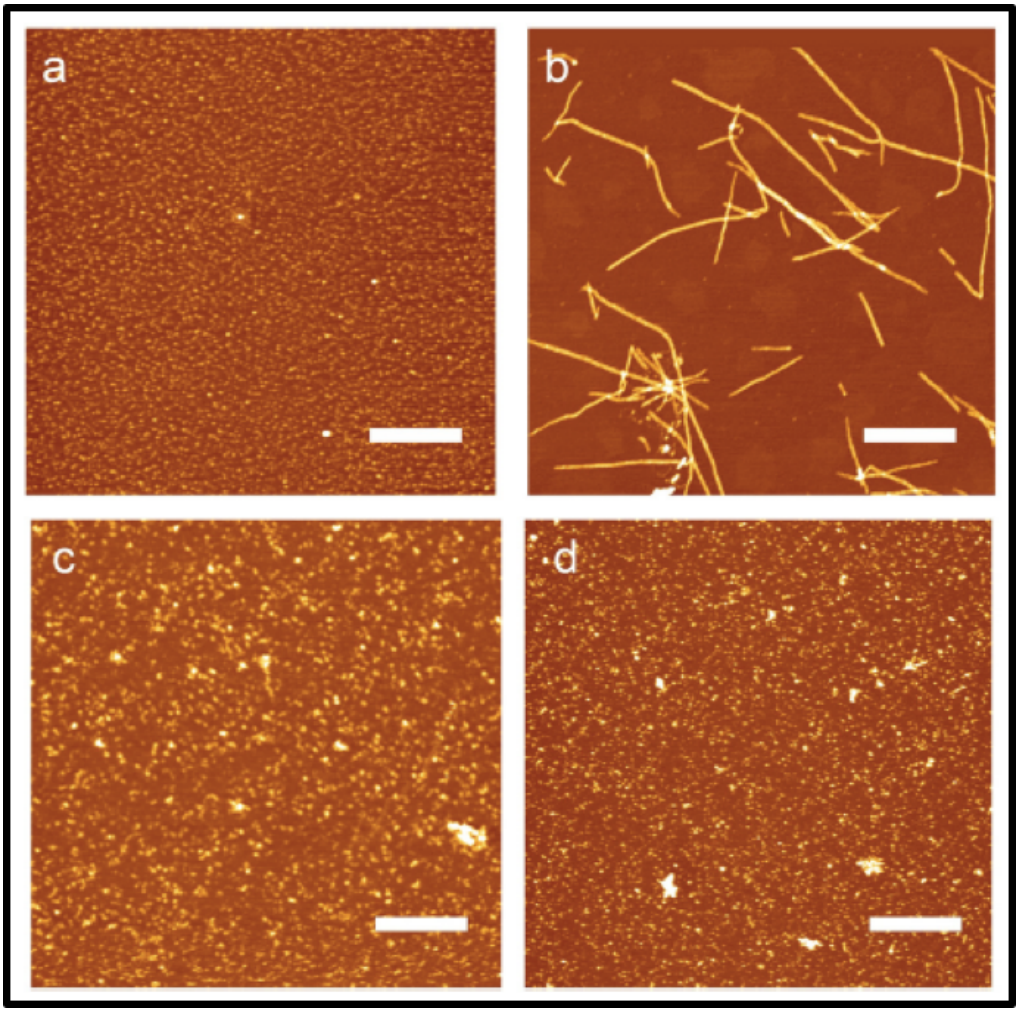


*Figure 12. AFM microscopy of time points of Aβ1-40 kinetic either alone or in presence of Hsp60. A. Aβ1-40 50 uM at time zero of the aggregation kinetic, showing absence of aggregates. B. Aβ1-40 50 uM after 24 hours of aggregation kinetic showing the presence of fibers. C. Aβ1-40 50 uM incubated with Hsp60 2 uM at initial time of aggregation kinetic showing the presence of small oligomers due to the heptameric and tetradecameric structures of Hsp60. D. Aβ1-40 50 uM incubated with Hsp60 2 uM after 24 hours of aggregation kinetic showing a morphology similar to panel c, suggesting the absence of amyloid aggregates. Scale bars: 1 um, Z-range 7 nm (a-c) or 9.6 nm (d) [105].*

- *Effect of Hsp60 on Aβ1-40 aggregation pathway in a cell free model*

I further characterized Hsp60-Aβ protein-protein interaction using size-exclusion chromatography. Particularly, with this technique I tested the working hypothesis that the effect of Hsp60 on $A\beta_{1-40}$ aggregation kinetic was irreversible, thus resulting in a loss of aggregation propensity. In detail, size exclusion chromatography (SEC-HPLC) is a both qualitative and

quantitative technique that allows to separate components of a sample mixture by size. Particularly, the "quality" of the size is given by the retention time (R.T.), expressed in minutes, and the "quantity" is given by the area under curve of each specific peak of the chromatogram. Moreover, this technique allows to calculate the precise molecular weight of each peak by comparing data obtained with the chromatogram of a standard mixture of proteins with known molecular weight. Therefore, it was possible analyze the distribution of different aggregates of $A\beta_{1\text{-}40}$ that were formed after the aggregation kinetic either in absence or upon Hsp60 treatment. Furthermore, to separate higher molecular weight oligomers from monomers allowed to employ isolated fractions for further analysis, as this technique did not alter the stability of amyloid beta peptide [115]. However, with this technique was not possible to observe aggregates with the size of fibers, as the pores of the stationary phase did not allow the passage of these aggregates through the column. Therefore, a valid approach used to estimate the amount of aggregates formed was to compare the area under the curve of the monomeric fractions at two time points of the aggregation kinetic (i.e. 0 and 24 hours) and to calculate the formation of fibers as the complementary of the monomeric fraction.

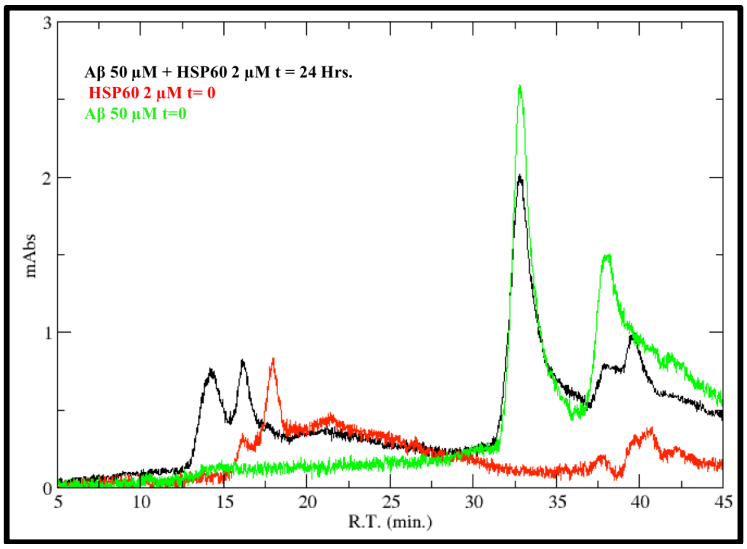


*Figure 13. Comparison between chromatograms after SEC-HPLC injections of Aβ1-40 50 µM (green line), Hsp60 2 µM (red line) and Aβ1-40 50 µM co-incubate with Hsp60 2 µM (black line).*

In detail, I analyzed and subsequently isolated by SEC-HPLC $A\beta_{1-40}$ fractions either incubated or not with Hsp60. As controls, I injected a sample of monomeric $A\beta_{1-40}$ and Hsp60 to estimate the retention time of both proteins alone. As summarized in figure 13, the injection of freshly prepared $A\beta_{1-40}$ monomers (green line, figure 13), produced a chromatogram characterized by a peak with a retention time around 33 minutes. Furthermore, I confirmed that to inject Hsp60 produced peaks around minutes 14 and 15.5 minutes (red line, figure 13). As we compared this data to a chromatogram of $A\beta_{1-40}$ incubated with Hsp60 under pro-aggregating conditions (black peak, figure 13), we observed that the peak corresponding to the monomeric fraction of Aβ was very similar either in quality that in quantity to the untreated control, thus further confirming the anti-aggregating effect of Hsp60 on $A\beta_{1-40}$. Moreover, I wanted to test the misfolding ability of $A\beta_{1-40}$ that has been exposed to Hsp60, after SEC-HPLC purification. This test for simplicity has been referred as "aggregation assay" (figure 14). Particularly, I prepared two samples: a sample of $A\beta_{1-40}$ never exposed to Hsp60 and a sample incubated with Hsp60. Both samples are incubated under pro-aggregating conditions (24 hours, 37 °C and 200 rpm) prior to the injection into the HPLC system. For both samples, fractions around 33 minutes are collected and incubated for 20 hours under the same conditions as prior to HPLC injection. Subsequently, I tested with ThT assay in both samples ($A\beta_{1-40}$ and $A\beta_{1-40}$ exposed to Hsp60 before SEC-HPLC purification) the presence of aggregates, as ThT emission is an indirect measure for fibrillary aggregates. Figure 14 summarizes results obtained from purified fractions of $A\beta_{1-40}$ pre-exposed (blue line) or not (red line) to Hsp60 for 24 hours and subsequently incubated for further 20 hours under pro-aggregating conditions. Data obtained suggests that Aβ, once exposed to Hsp60, is not able to aggregate neither after Hsp60 has been removed. Conversely, chromatographic fractions purified from a sample of $A\beta_{1-40}$ gives ThT fluorescence positivity after 20 hours of incubation, due to fiber formation.

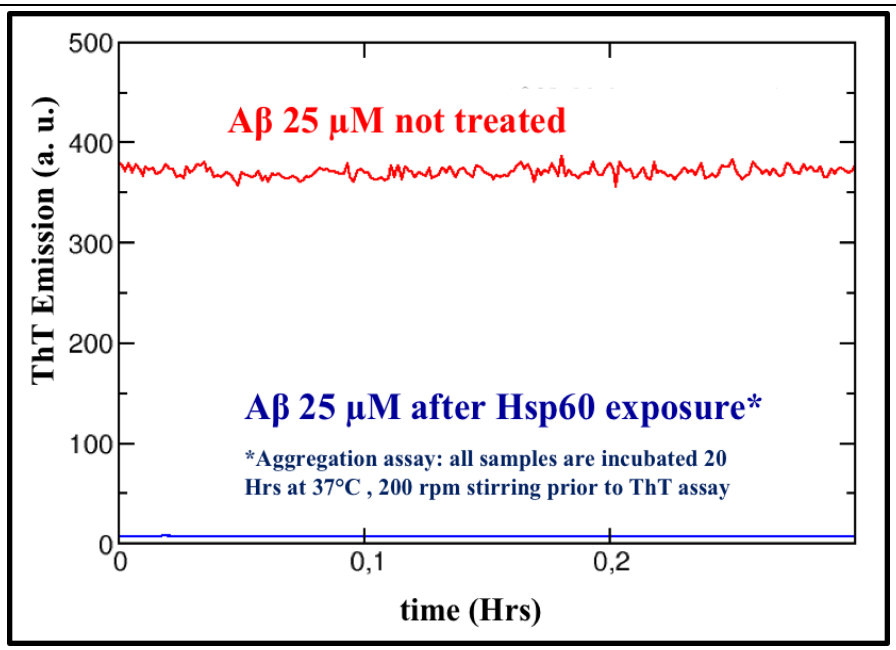


*Figure 14. ThT assay of Aβ1-40 samples either treated (blue line) or not (red line) with Hsp60 2 µM, prior to HPLC injection and 20 hours of incubation at 37 ° C and 200 rpm (aggregation test) prior to the assay.*

- *Effect of Hsp60 on Aβ1-42 aggregation pathway in a cell free model*

To further validate the anti-aggregating effect of Hsp60, I used $A\beta_{1-42}$ as an alternative model of amyloid aggregation. Differently from $A\beta_{1-40,}$ the aggregation kinetic of this peptide was much faster and, therefore, there was not lag phase observed with the ThT assay, as observed in $A\beta_{1-40}$, due to the immediate formation of seeds and aggregates. As summarized in figure 15, there is preliminary evidence suggesting an anti-aggregating effect of Hsp60 also on a much more aggressive model of aggregation, such as $A\beta_{1-42.}$ However, further investigation is needed to validate the effect of Hsp60 on $A\beta_{1-42}$ aggregation kinetic.

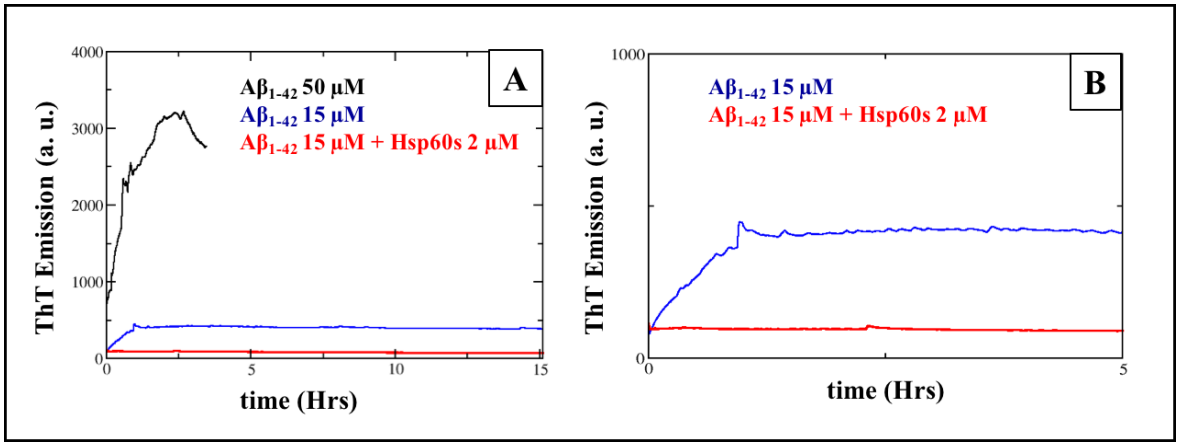


*Figure 15. Biophysics analysis of Hsp60 effect on Aβ1-42. A. ThT assay of Figure Aβ1-42 50 µM (black line) suggests that the aggregation is too fast compared to Aβ1-40 and therefore peptide concentration is lowered until 15 µM (blue line). ThT assay of Aβ1-42 treated with Hsp60 suggests that the chaperon inhibits Aβ1-42 aggregation despite the high propensity to aggregate. B. Highlight of first 5 hours of kinetic between Aβ1-42 and Hsp60 shown in figure A to better observe the antiaggregating effect of Hsp60.*

- *Effect of GroEL on Aβ1-42 aggregation pathway in a cell free model*

I further tested if results obtained with human Hsp60 were reproducible with the bacterial homolog, GroEL. In detail, as summarized in figure 16, I tested if under the same conditions used for human Hsp60, GroEL was also an effective inhibitor of $A\beta_{1\text{-}40}$ aggregation kinetic. I addressed my working hypothesis using ThT and CD assays. Figure 16A shows the intensity of emission of ThT for $A\beta_{1\text{-}40}$ either not exposed or exposed to GroEL and data suggested that in these conditions ($A\beta_{1\text{-}40}$ 50 µM and GroEL 2 µM), there was not an inhibition of Aβ aggregation. One possible explanation of the phenomenon is that the conditions used do not allow an effective inhibition of $A\beta_{1\text{-}40}$ aggregation. Therefore, I tested a different condition based on isothermal titration calorimetry data from our collaborators (unpublished data, not shown). Panel B and C of figure 16 summarize the results obtained testing $A\beta_{1\text{-}40}$ 25 µM and GroEL 7 µM (red line), comparted to $A\beta_{1\text{-}40}$ 25 µM alone (blue line). Briefly, ThT assay showed the effect of GroEL in increasing the lag phase of Aβ aggregation, even though the kinetic was not completely blocked. This data was consistent with CD data summarized in panel C of figure 16.

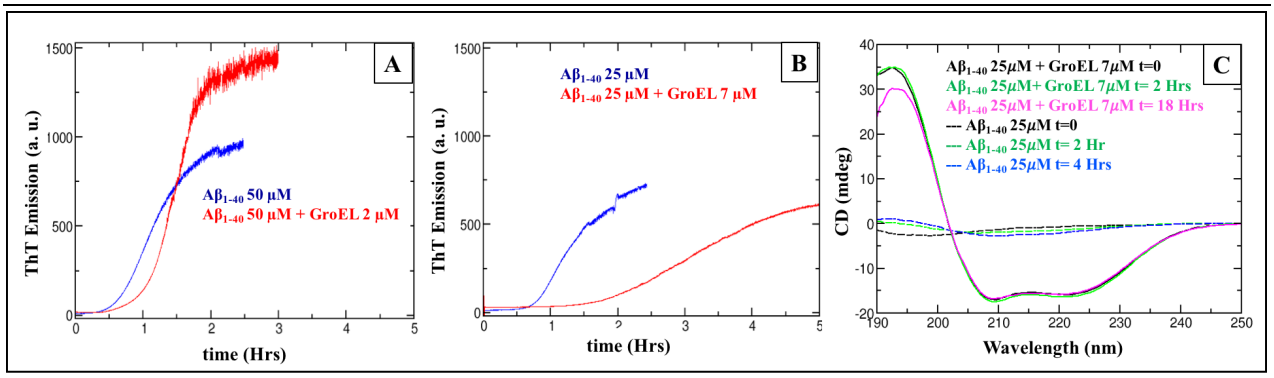


*Figure 16. GroEL effect on $A\beta_{1-40}$ aggregation kinetic characterized by ThT assay and CD analysis. A. ThT assay of $A\beta_{1-40}$ 50 µM exposed to GroEL 2 µM (red line) compared to $A\beta_{1-40}$ 50 µM untreated (blue line). B. ThT assay of $A\beta_{1-40}$ 25 µM exposed to GroEL 7 µM (red line) compared to $A\beta_{1-40}$ 25 µM untreated (blue line). C. Summary of CD spectra measured at time points of the aggregation kinetic of $A\beta_{1-40}$ exposed to GroEL: 0 (black line; 2 hours (green line); 18 hours (magenta line). Data was compared to $A\beta_{1-40}$ kinetic: 0 (black dotted line); 2 hours (green dotted line); 4 hours (blue dotted line).*

## 2. Characterization of the protective effect of Hsp60 against Aβ toxicity *in vitro*

- *Co-expression of APP and Hsp60 in vitro: 7PA2/H60 cell line design and validation*

Results discussed in the previous section suggest a direct inhibitory effect of Hsp60 on Aβ aggregation. Therefore, I wanted to test the working hypothesis that Hsp60 has a direct effect on Aβ cascade using a more complex model. Therefore, I used as a model a cell line overexpressing the Swedish variant of APP (7PA2 cells) and that is known to release human Aβ oligomers in the culture medium, that are known to be toxic if injected *in vivo* [116,117]. Therefore, this has been used as a good model to test the effect of Hsp60 on Aβ oligomers *in vitro*. Figure 17 summarizes the experimental design for the study of Hsp60-Aβ protein-protein interaction *in vitro*. Briefly, I transfected 7PA2 cell line using a pCMV6 plasmid either empty, as a control, or encoding for human Hsp60 protein 24 hours after cells were seeded on a multiwall plate at desired confluency. Optimal transfection conditions were tested using either different volumes of lipofectamine 2000 (7, 9, 12 µL) or different plasmid concentrations (1,3,5,7 µg). Condition tested are summarized in table 2.

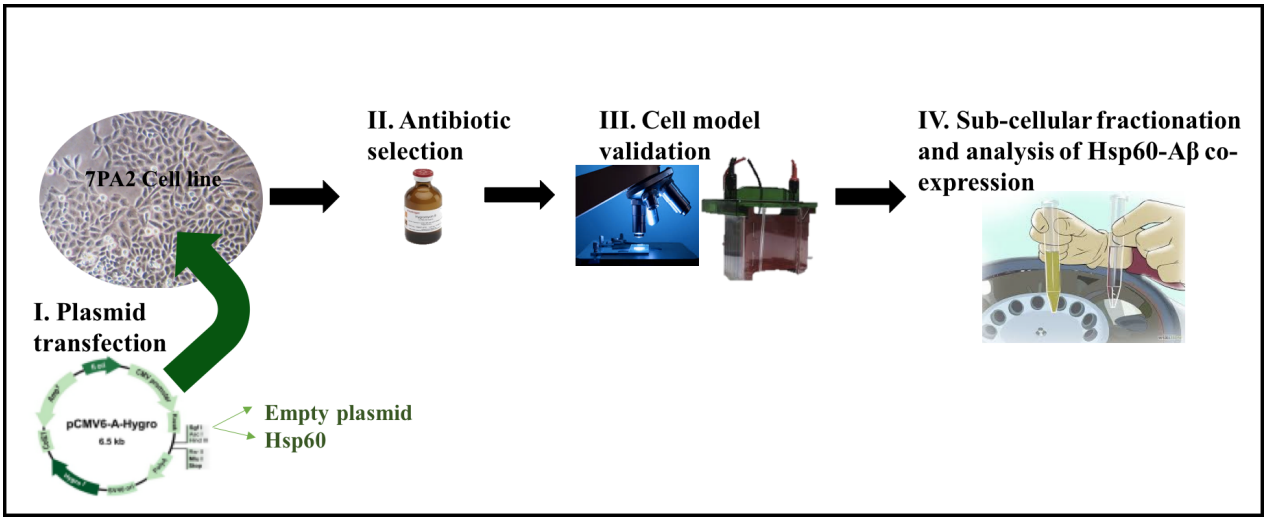


*Figure 17. Experimental design for in vitro overexpression of Hsp60 on 7PA2 cell line that overexpresses APP. After transfection (I), cell will be selected with hygromycin (II) and validated by WB and IIC (III). Subsequently, sub-cellular fractionation and analysis of Hsp60-Aβ co-expression in subcellular compartments will be also tested (IV).*

Despite the conditions chosen (different volumes of lipofectamine or different quantities of cDNA), all transfections were blocked after 5 hours with DMEM 10% FBS and cells kept for 24 hours without antibiotics to allow cells to recover.

*Table 2. Summary of condition tested to optimize cell transfection.*

| Conditions | 1 | 2 | 3 | 4 | 5 |
|---|---|---|---|---|---|
| Cell line | CHO/7PA2 | CHO/7PA2 | CHO/7PA2 | CHO/7PA2 | CHO/7PA2 |
| Lipofectamine 2000 (µL) | 0 | 7 | 9 | 12 | - |
| Type of plasmid | pCMV6-Empty/ pCMV6-hHsp60 | pCMV6-Empty/ pCMV6-hHsp60 | pCMV6-Empty/ pCMV6-hHsp60 | pCMV6-Empty/ pCMV6-hHsp60 | pCMV6-Empty/ pCMV6-hHsp60 |
| Plasmid concentration (µg) | 0 | 1 | 3 | 5 | 7 |

Transfection efficiency was verified using both western blotting (WB, figures 19, 20) and immunocytochemistry (ICC, figures 21-23). For both experimental approaches, detection and

quantification of recombinant Hsp60 protein was verified by a specific antibody for the c-terminus tag (DDK antibody) and by a specific antibody for detecting total Hsp60 levels. Some of the conditions that have been tested on both CHO and 7PA2 cell lines are summarized in a representative immunocytochemistry presented in figure 18. Particularly, in blue are stained nuclei with DAPI and in green is strained the recombinant protein that has been overexpressed after plasmid transfection, using DDK antibody. Based on these preliminary results, 3 µg cDNA and 7 µl Lipofectamine 2000 were used to create the cellular model which co-expressed APP and Hsp60, that will be referred in the following text as "7PA2/H60" cell line.

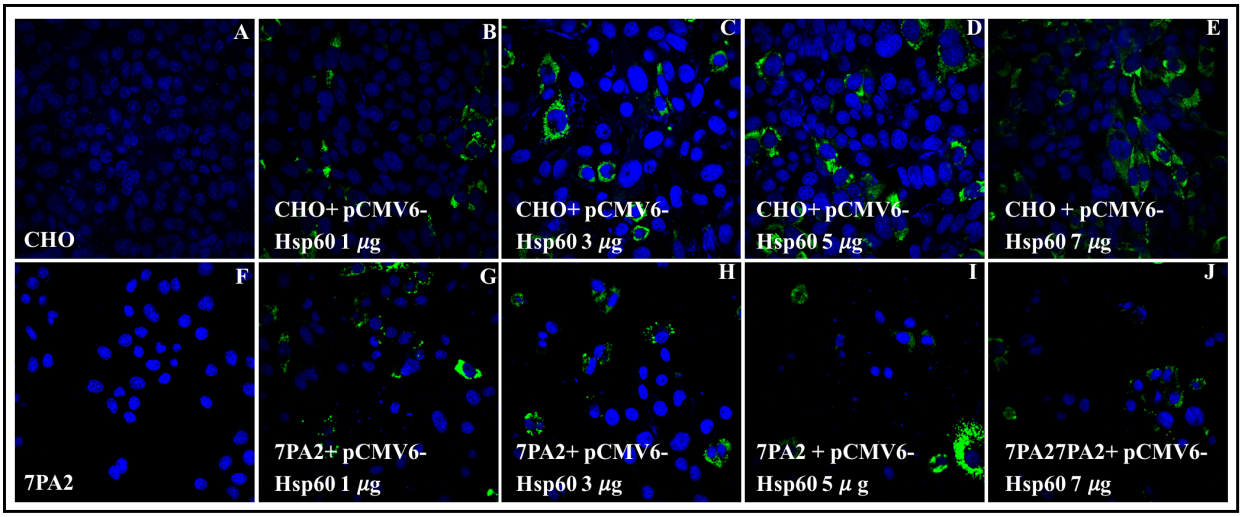


*Figure 18. Immunocytochemistry (ICC) of CHO and 7PA2 with pCMV6 plasmid encoding from recombinant Hsp60. A-E. CHO cell line transfected with increasing concentrations of pCMV6-Hsp60 plasmid (1,3,5,7 µg). F-J. 7PA2 cell line transfected with increasing concentrations of pCMV6-Hsp60 plasmid (1,3,5,7 µg). Antibodies: DAPI, blue = nuclei; DDK, green= recombinant Hsp60.*

To select a transient cell line that co-expresses both APP and Hsp60 proteins, I characterized the minimum concentration of antibiotics that was toxic for cells that did not have the plasmid, as both plasmids that have been used to create the cell lines encoded for specific antibiotic resistance. Particularly, the plasmid responsible for APP expression in 7PA2 cell line expressed also the resistance for neomycin (or G418 antibody), while the plasmid encoding for Hsp60 expressed also

hygromycin resistance. Based on kill curves obtained with CHO and 7PA2 cells exposed for 1 week to serial concentrations of antibiotics (data not shown), 7PA2/H60 cell line was obtained using G418/hygromycin B 0.6 mg/0.6mg in DMEM, 10 % FBS, 1% p/s. Positive transfection was also tested with WB blotting technique after one week and one month of transfection, as summarized in figure 19. Particularly, I verified the overexpression of APP by WB using 6E10 antibody, which stained for APP/Aβ in 7PA2 and 7PA2/H60 cell lines, compared to naïve CHO cells. Moreover, I confirmed the overexpression of recombinant Hsp60 only in 7PA2/H60 cell line using a specific antibody anti-tag expressed in the recombinant protein (DDK) and I further validated the co-localization of the signal obtained with DDK and Hsp60, thus confirming that the overexpressing recombinant is Hsp60 (Figure 19, A).

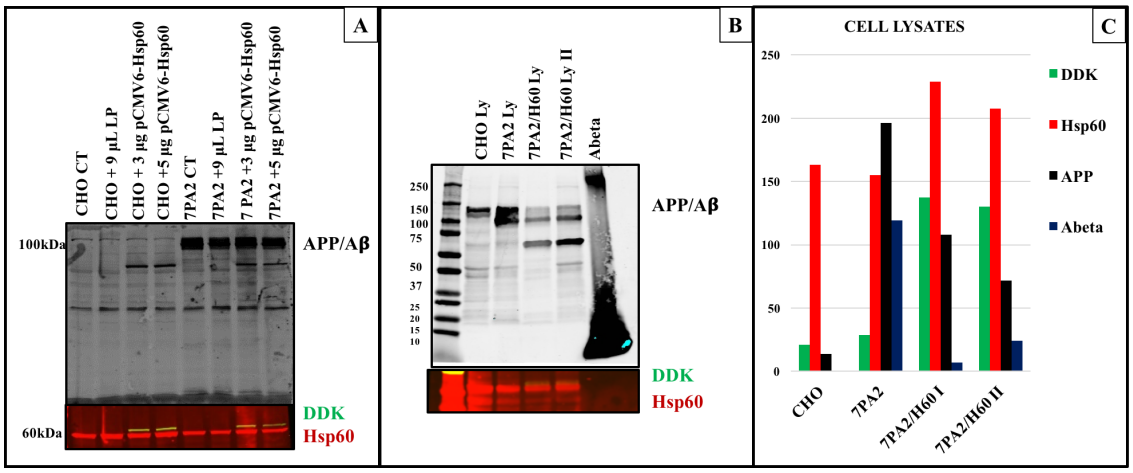


*Figure 19. Western blotting (WB) validation of 7PA2/H60 cell line. A. representative WB of total lysates of CHO, 7PA2 and 7PA2/H60 confirming that all cell lines are positive to total Hsp60 antibody, that only 7PA2/H60 is positive to DDK antibody for recombinant Hsp60 and that only 7PA2 and 7PA2/H60 are positive to 6E10 antibody (APP/Aβ). B. representative WB of total lysates of CHO, 7PA2 and 7PA2/H60 after 1 week and after 1 month of transfection (7PA2/H60 Ly II) using 6E10 (APP/Aβ), DDK and Hsp60 antibodies confirms the validation of 7PA2/H60 cell line. C. Quantification of WB bands presented in B.*

Subsequently, I confirmed the expression of all proteins of interest (APP/Aβ, total and recombinant Hsp60) also after a long exposure (1 month, figure 19 line "7PA2/H60 Ly II") to toxic concentrations of selection antibody (figure 19, B). I further quantified the levels of DDK, Hsp60,

APP (considering the lower band in the 130 KDa range) and Aβ ( 4 KDa band), either after one week ("7PA2/H60 I" line, panel B and C of figure 19) or after one month (7PA2/H60 II line, panel B and C of figure 19) of transfection, using ImageJ, as summarized in figure 19C. Overall, data suggests a successful overexpression of Hsp60 in 7PA2 cells already overexpressing APP protein.

I further validated the overexpression of APP and Hsp60 in 7PA2/H60 cell line comparing the transfection with cells transfected with an empty plasmid, as summarized in figure 20. Particularly, panel A is a representative western blotting of total cell lysates from CHO, 7PA2, 7PA2 transfected with empty plasmid and 7PA2/H60 cell lines to test the expression of APP, total Hsp60 and recombinant Hsp60. The quantification of the bands for Hsp60, DDK and APP proteins normalized to β-actin is summarized in panel B. This data validated the co-expression of APP/Aβ and Hsp60 in the novel cellular model referred as 7PA2/H60 cell line.

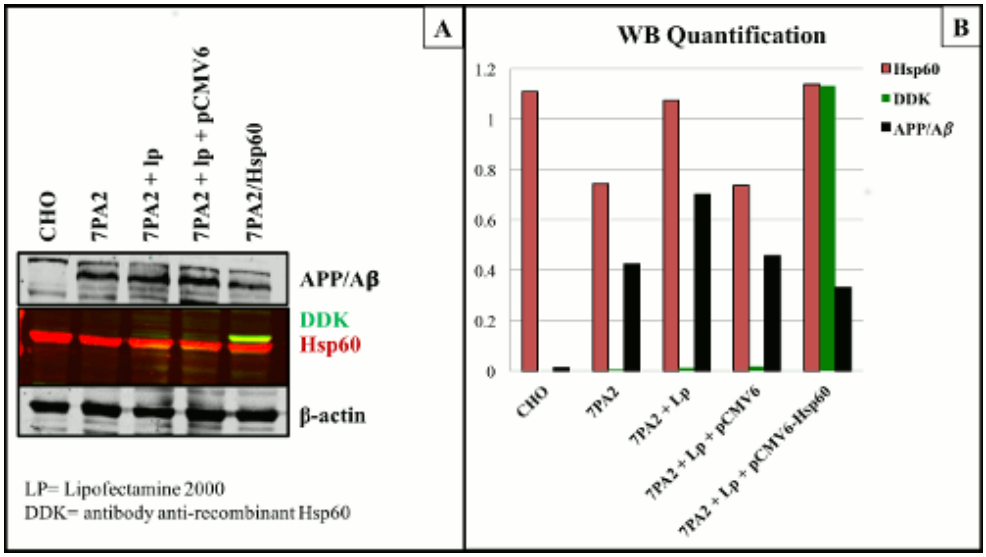


*Figure 20. Western blotting (WB) validation of 7PA2/H60 cell line. A. representative WB of CHO, 7PA2, 7PA2 transfected with empty pCMV6 plasmid and 7PA2/H60, validating that 7PA2/H60 cell line co-expresses APP and recombinant Hsp60. B. quantification of blot presented in panel A, using ImageJ.*

In parallel experiments, I characterized 7PA2/H60 cell line using immunocytochemistry (ICC). Particularly, I validated APP/Aβ expression of in 7PA2 and 7PA2/H60 cell lines, compared to CHO

as a control, using 6E10 antibody for APP/Aβ detection. Furthermore, I validated the expression of total Hsp60 in all cell lines used, CHO, 7PA2 and 2PA2/H60 lines, as Hsp60 is a ubiquitous protein. Finally, I confirmed the expression of recombinant Hsp60 in 7PA2/H60 cell line using DDK antibody and confirmed the co-localization with Hsp60 antibody. Representative ICC data is summarized in figure 21, 22 and 23.

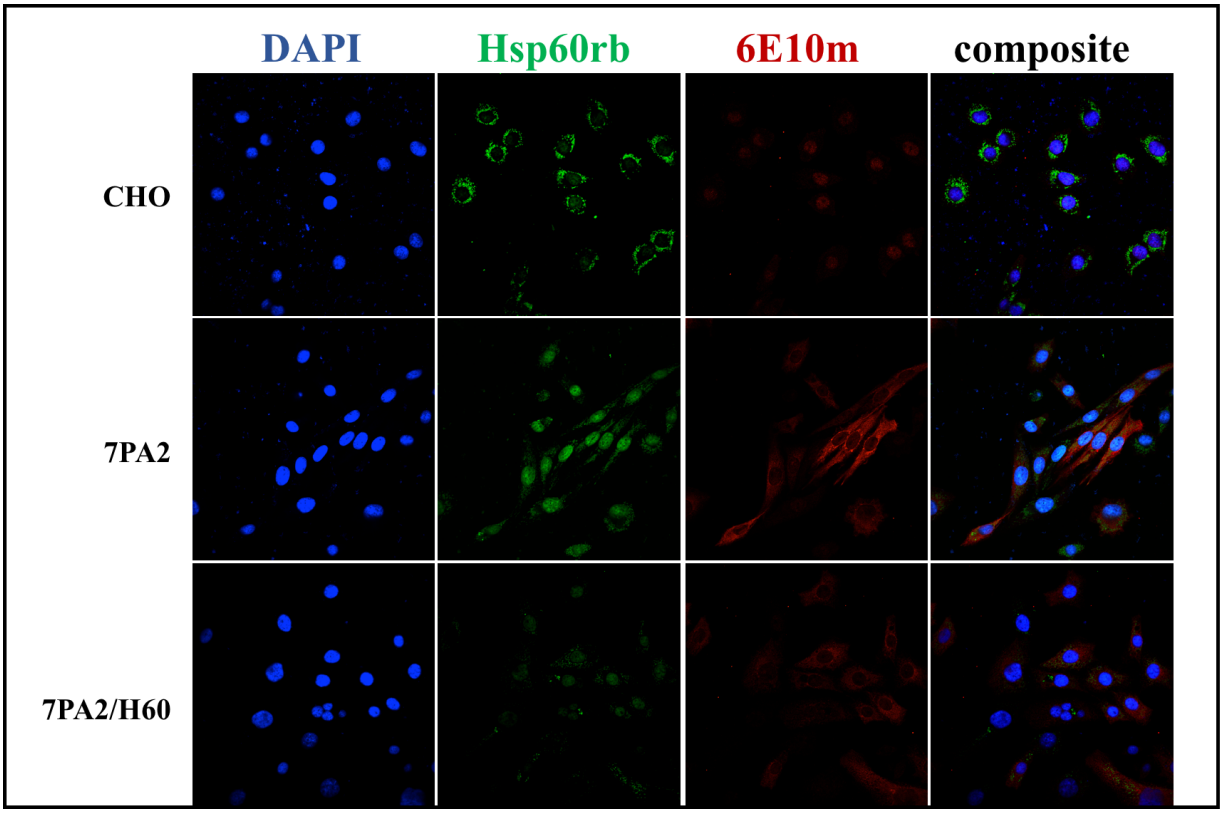


*Figure 21. ICC validation of 7PA2/H60 cell line. Data confirms that Hsp60 is expressed in all cell lines as this protein is ubiquitous and that the expression of APP is only in 7PA2 and 7PA2/H60 cell lines. DAPI, blue= nuclei; Hsp60rb, green= total Hsp60; 6E10ms, red= APP/Aβ.*

Particularly, figure 21 is a representative immunocytochemistry of CHO, 7PA2 and 7PA2/H60 cell line stained with DAPI for nuclei detection (blue channel), Hsp60 antibody for total Hsp60 detection (green channel) and 6E10 antibody (red channel) for APP/Aβ detection, showing that only 7PA2 and 7PA2/H60 cell lines were positive for 6E10 antibody and therefore expressed APP protein. Figure 22 is a representative immunocytochemistry of CHO, 7PA2 and 7PA2/H60 cell line

stained with DAPI for nuclei detection (blue channel), Hsp60 antibody for total Hsp60 detection (green channel) and DDK antibody (red channel) for recombinant Hsp60 detection, showing that only 7PA2/H60 cell line was positive for DDK antibody and therefore expressed recombinant Hsp60 protein.

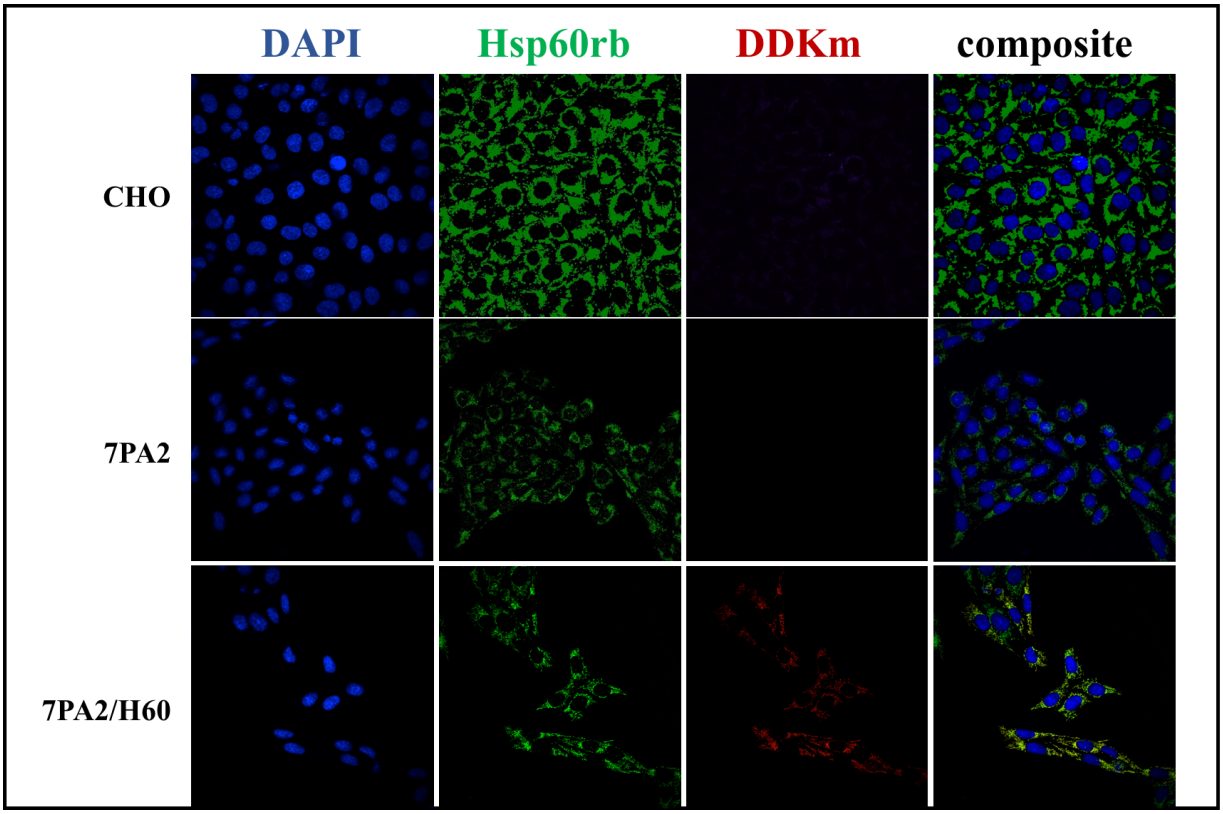


*Figure 22. ICC validation of 7PA2/H60 cell line. Data confirms the expression of Hsp60 in all cell lines and only in 7PA2/60 the expression of recombinant Hsp60 as confirmed by the co-localization of total Hsp60 and DDK antibodies. DAPI, blue= nuclei; Hsp60rb, green= total Hsp60; DDKms, red= recombinant Hsp60.*

Figure 23 is a representative immunocytochemistry of CHO, 7PA2 and 7PA2/H60 cell line stained with DAPI for nuclei detection (blue channel), DDK antibody for recombinant Hsp60 detection (green channel) and 6E10 antibody for APP/Aβ detection (red channel), showing that only 7PA2/H60 cell line co-expressed both APP and recombinant Hsp60 proteins.

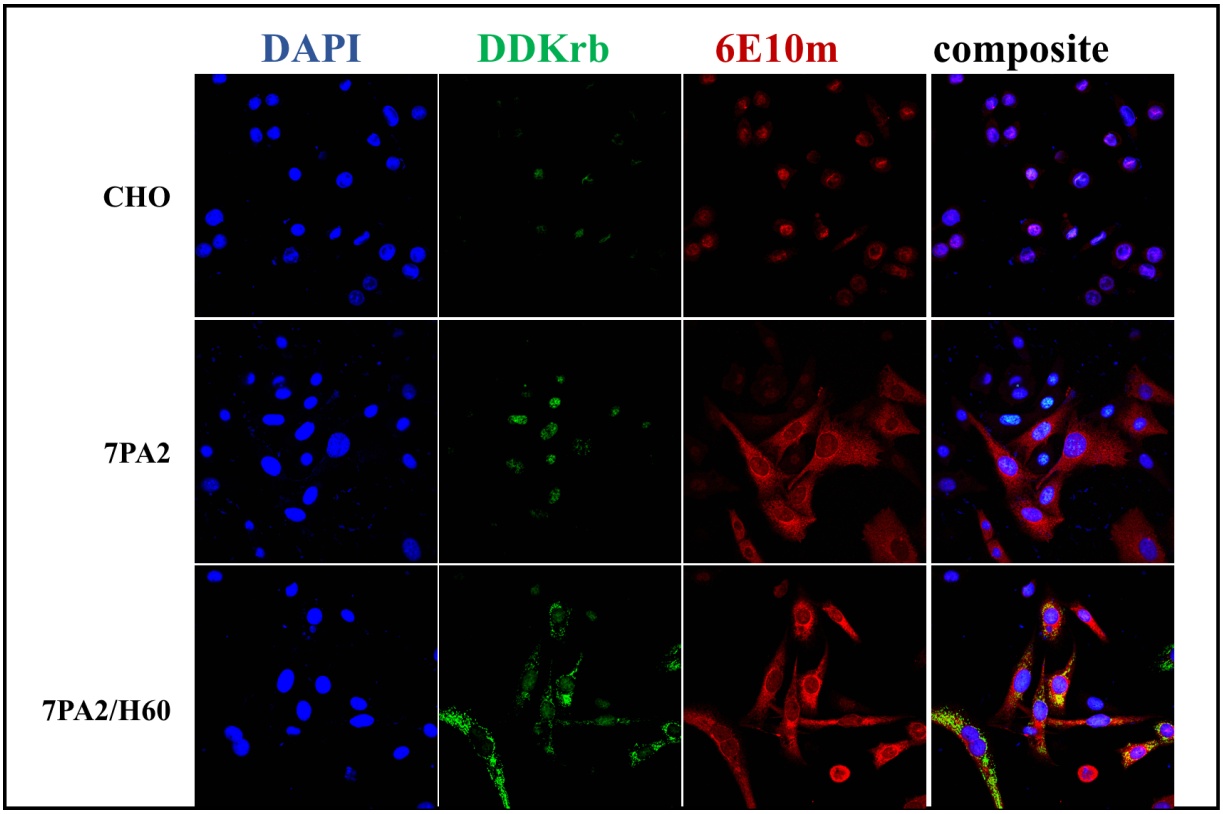


*Figure 23. ICC validation of 7PA2/H60 cell line. Data confirms the expression of both APP and recombinant Hsp60 in 7PA2/H60 cell lines. DAPI, blue= nuclei; DDKrb, green= recombinant Hsp60; 6E10ms, red= APP/Aβ.*

- *Investigating the co-expression of APP and Hsp60 in sub cellular compartments*

The novel cellular model that co-expressed both APP and Hsp60 proteins allowed to investigate the effect of Hsp60 on Aβ cascade *in vitro*. Particularly, I investigated the working hypothesis that Hsp60 as an effect on APP and Aβ production in different sub-cellular compartments: whole cell, mitochondria and extracellular compartment. The rationale of this investigation was based on the known toxic localization of Aβ oligomers into the mitochondria and the known protective action of Hsp60 in the mitochondria [118,119]. Moreover, the following experiments aimed to support the beneficial effect on enhancing the chaperone machinery as a potential approach for future therapies for Alzheimer's disease. As the goal is to investigate the functional interaction between Aβ and Hsp60 in sub-cellular compartments, I first validated the protocols for mitochondria isolation and extracellular compartment purification. In detail, mitochondria isolation has been done using

Qproteome mitochondria isolation kit (Qiagen), based on the manufacturer protocol. The purity of isolated mitochondria has been validated by western blotting in all three cells lines of interest (CHO, 7PA2 and 7PA2/H60 cell lines) and the protein validation is summarized in figure 24 with a representative western blotting. Particularly, the comparison of total cell lysates with cytoplasmic and mitochondria fractions allowed to observe an enrichment in SOD2 positive band in the mitochondria fraction, as SOD2 is a specific enzyme expressed in mitochondria. Both Hsp60 and SOD2 bands were normalized to β-actin, used as loading control.

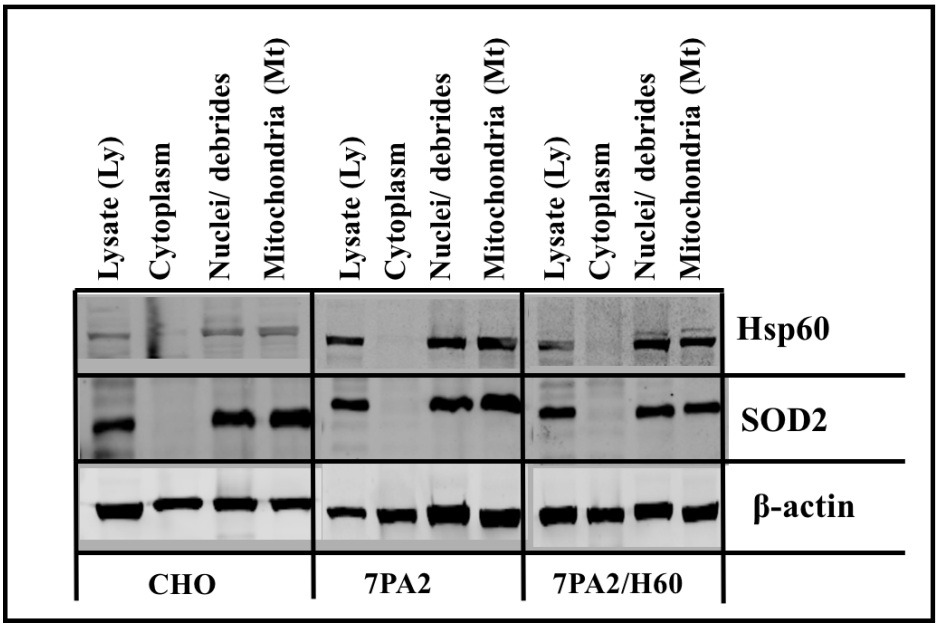


*Figure 24. WB validation of mitochondria and cytosolic fractions of CHO, 7PA2 and 7PA2/H60 using Qproteome mitochondria isolation kit. Data confirms that Hsp60 and SOD2 are compartmentalized in the mitochondria of all cell lines.*

Moreover, as it is known from literature that 7PA2 cells secrete Aβ into the media and that once released [108, 117, 120], it aggregates into toxic oligomers, I optimized the protocol from media concentration from CHO, 7PA2 and 7PA2/H60 cell line to test the working hypothesis that Hsp60 has a direct influence on Aβ release in the media. Figure 25 summarizes the experimental design applied for media isolation.

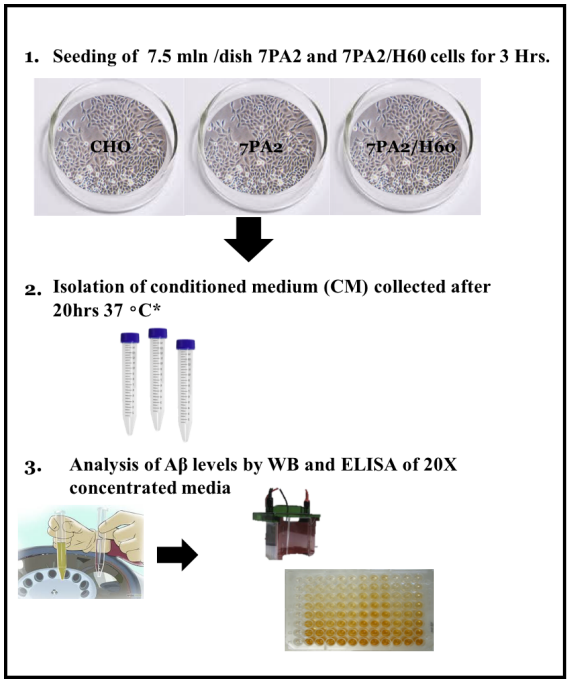


*Figure 25. Experimental design of extracellular fractions isolated from CHO, 7PA2 and 7PA2/H60 cell lines. 1. Cell are first seeded in a Petri dish in regular media and after 3 hours, all media is replaced with serum free and antibiotics free DMEM and cells left in the incubator for 20 hours. 2. After 20 hours, conditioned media (CM) is collected and concentrated up to 20 times. 3. All concentrated fractions are analyzed with WB and ELISA.*

Briefly, I first seeded CHO, 7PA2 and 7PA2/H60 cell lines in Petri dishes at about 90% confluency and allowed cells to attach for 3 hours in regular media. After 3 hours, I washed and left all cells in serum-free, antibiotics-free DMEM media. After 20 hours in the incubator, I removed the media and I either concentrated media up to 20 times for analysis of Aβ levels via WB and ELISA or either used for toxicity assay (described in the following chapter).

The characterization using western blotting of conditioned media (CM) isolated and concentrated from CHO, 7PA2 and 7PA2/H60 cell lines is summarized in figure 26. Particularly, I tested the levels of APP/Aβ using the specific anti amyloid antibody 6E10. As expected, only 7PA2 and 7PA2/H60 cells are positive to 6E10 antibody either in lysates and CM.

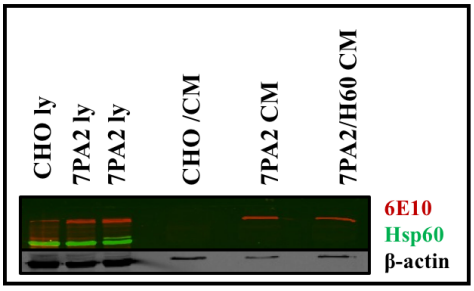


*Figure 26. WB validation of conditioned media (CM) fractions of CHO, 7PA2 and 7PA2/H60 cell lines, compared to total lysates. 6E10 antibody confirms the positivity to APP/Aβ proteins only in 7PA2 and 7PA2/H60 media. Hsp60 antibody confirms the presence of Hsp60 protein only in total lysate fractions.*

After I validated all protocols for mitochondria and extracellular environments, I investigated the effect of Hsp60 overexpression on APP/Aβ in whole cells, cytoplasm, mitochondria and extracellular compartments. A representative western blotting of whole cell lysates of CHO, 7PA2 and 7PA2/H60 cell lines using 6E10 antibody for APP/Aβ fragments, DDK for recombinant Hsp60 and Hsp60 for total Hsp60 is presented in figure 27 A. Quantification of the bands is summarized in panel B of figure 27.

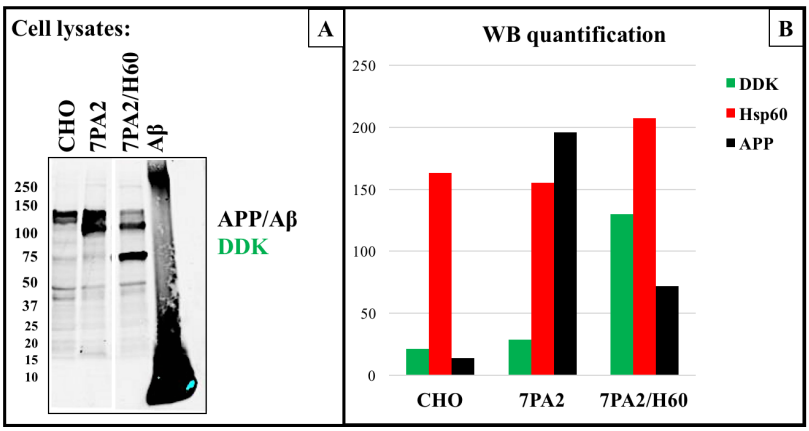


*Figure 27. Co-expression of Hsp60 and APP/Aβ proteins in whole cell compartment. A. representative WB of total cell lysates of CHO, 7PA2 and 7PA2/H60 cell lines confirms the co-expression of Hsp60 and APP and suggests a reduction in APP expression as Hsp60 is overexpressed. B. Quantification of WB using ImageJ.*

Overall, data suggested that the overexpression of Hsp60 reduced APP levels in total cell lysates that, however, was not significant after further investigations (data not shown).

Furthermore, I tested levels of total Hsp60, recombinant Hsp60 and APP/Aβ levels in mitochondria, cytoplasm and extracellular environments (referred as conditioned media or CM). As summarized in figure 28, there was not a significant reduction in APP levels in 7PA2/H60 cell line compared to 7PA2 cell line. This data suggested that to overexpress Hsp60 might not have a direct effect on APP protein, despite it was observed a slight reduction of APP levels in 7PA2/H60 cell line.

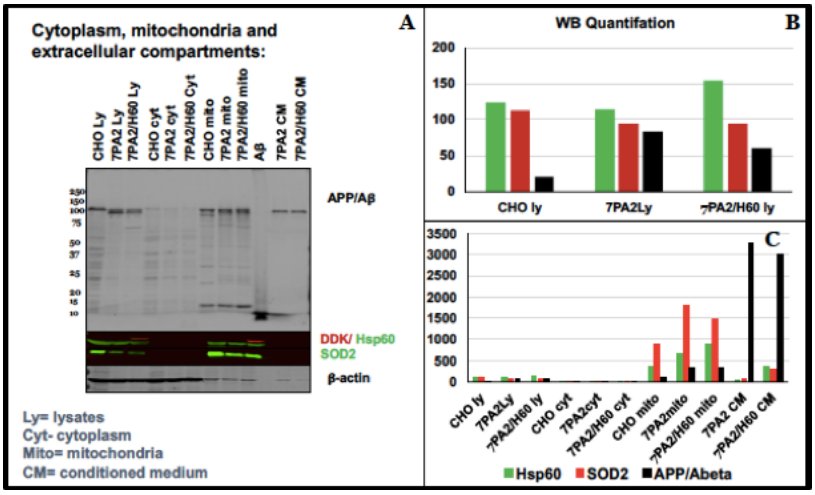


*Figure 28. Co-expression of Hsp60 and APP/Aβ proteins in cytoplasm, mitochondria and extracellular compartment. A. representative WB of the Comparison between total lysates, mitochondria and media (CM) compartments of CHO, 7PA2 and 7PA2/H60 cell lines suggests that Hsp60 overexpression reduces the amount of APP in all compartments investigated. B., C. Quantification of WB bands presented in panel A using ImageJ.*

However, as Aβ levels in both 7PA2 and 7PA2/H60 cell lines were in the order of picograms, it was challenging to detect the 4.5 KDa band of Aβ peptide via WD, especially in the conditioned media. Indeed, ELISA has been used as more sensitive technique allowing to detect low concentrations of Aβ peptide.

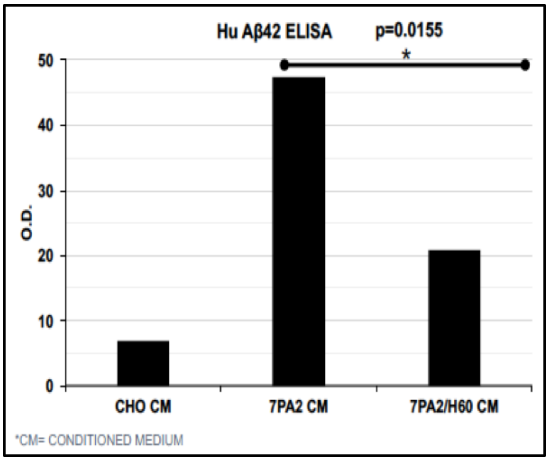


*Figure 29. Aβ1-42 ELISA of conditioned medium concentrated from CHO, 7PA2 and 7PA2/H60 cell lines suggests that Hsp60 overexpression reduces the amount of Aβ secreted in the medium*

Figure 29 shows the levels of $A\beta_{1-42}$ detected by ELISA in media concentrated from CHO, 7PA2 and 7PA2/H60 cell lines. Interestingly, Hsp60 overexpression reduced Aβ secreted levels in 7PA2/H60 media compared to 7PA2, as confirmed by ELISA assay. Overall, data suggested that to overexpress Hsp60 has an effect of a downstream cascade of APP, thus resulting in a reduction in Aβ levels in the extracellular compartment.

## 3. To determine Hsp60-dependent functional inhibition of downstream amyloid beta toxicity

As soon as Aβ is released by APP processing, toxic oligomers are formed and they are known to be responsible to bind synapses, cause neurotoxicity, and inhibit the functional process of long term potentiation, the mechanism involved in memory formation [53, 117]. Therefore, in this study, I tested the hypothesis that Hsp60 inhibits Aβ-driven neurotoxicity *in vitro*. Particularly, I investigated the effect of Hsp60 on naturally secreted oligomers, formed *in vitro* by 7PA2/H60 cell line (APP-Hsp60 co-expressing cell line) and I compared the effect to 7PA2, a cell line known to release toxic oligomers in the media [117]. The change in cytotoxicity was determined using LDH assay, as described in material and methods.

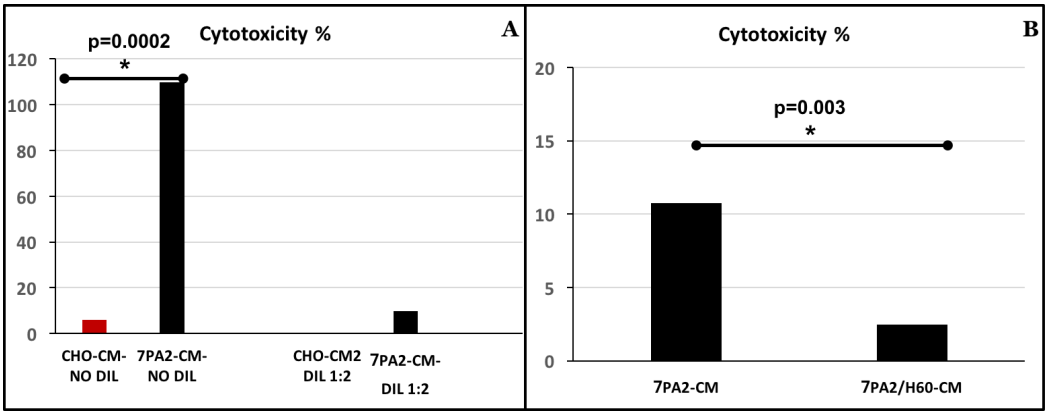


*Figure 30. Effect of Hsp60 on Aβ cytotoxicity. A. LDH assay of SHSY5Y after 24 hours' treatment, with two different doses of CHO and 7PA2 CM, confirms the increased toxicity of 7PA2 media due to the release of toxic Aβ oligomers. B. LDH of SH-SY5Y cells exposed 24 hours to conditioned medium extracted from 7PA2 and 7PA2/H60 cell lines (7PA2-CM or 7PA2/H60-CM) suggests that Hsp60 overexpression reduces the amount of Aβ secreted in the medium and cytotoxicity.*

The optimization of SH-SY5Y treatment of two different dilutions of conditioned media produced by naïve CHO and 7PA2 cell lines is summarized in Figure 30 A. As expected, 7PA2 cell line is toxic for neuroblastoma cells, because of the release in the media of cytotoxic oligomers. As shown in figure 30B, I compared the toxicity of 7PA2 media to 7PA2/H60 media and data suggested that 7PA2/H60 media is less toxic compared to 7PA2 media, thus suggesting an effect of Hsp60 on Aβ oligomer release or a reduction of toxic species released in the media. However, this approach cannot exclude that the phenomenon observed using 7PA2/H60 cell media was only related to a reduction of toxic Aβ, due to a reduced release, and therefore to a false negative due to a dilution effect. Therefore, I tested the effect of Hsp60 on preformed oligomers, as it has been extensively discussed that Aβ toxicity relies on its oligomeric conformation. To test the hypothesis that Hsp60 is protective against oligomer-induced cytotoxicity, I prepared Aβ oligomers using a protocol optimized in our laboratory [53], and I treated an aliquot with two different concentrations of Hsp60 in aseptic conditions. Moreover, to eliminate the activity of Hsp60, prior to each cell treatments, I heat-inactivated the chaperone by boiling the sample and I confirmed by western blotting the quality of oligomers using 4G8 antibody. Particularly, figure 31 shows a representative WB to confirm the

levels of Aβ oligomers in all conditions tested: oligomers freshly prepared, boiled, incubated 1 hour at 37 °C, or 3 hours, or incubated 1 hour and boiled. Furthermore, I tested the quality of oligomers also after exposure to Hsp60.

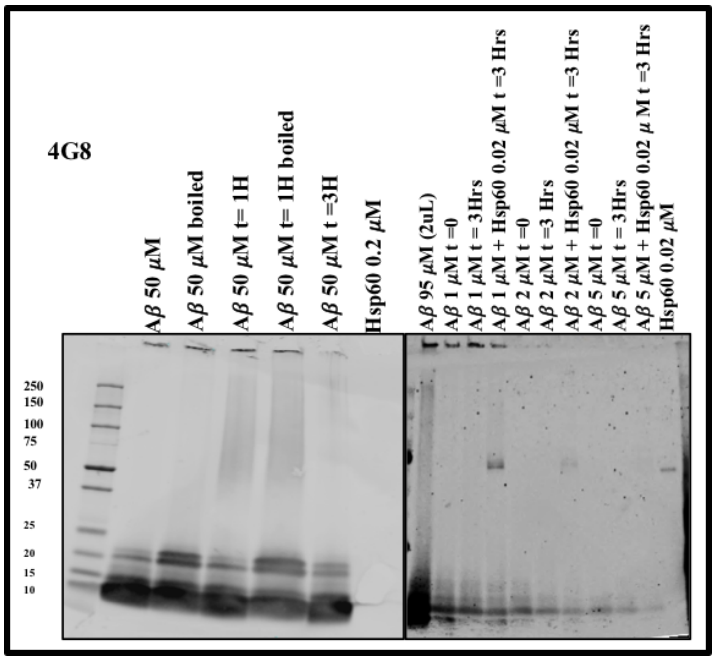


*Figure 31. WB characterization of preformed Aβ oligomers exposed to different conditions. Samples exposed to Hsp60 were incubated with Hsp60 for 1 hour at 37 °C and bold for 1 minute to heat inactivate Hsp60. The procedure did not alter the quality of preformed oligomers.*

Moreover, I tested the optimal concentration of Aβ oligomers that was toxic for SH-SY5Y and, as described in figure 32, Aβ oligomers were toxic either at 5 and 10 μM. Indeed, I decided to use Aβ 5 μM for testing changes in cytotoxicity upon Hsp60 treatment. As summarized in figure 33, I tested the effect of two different concentrations of Hsp60 on Aβ-induced toxicity. Particularly, I exposed Aβ oligomers to Hsp60 1 or 2 μM and I tested the toxicity of Hsp60 at the same condition as control. Sample were diluted 10 times and, therefore, in the graph are reported final concentrations administered to cells.

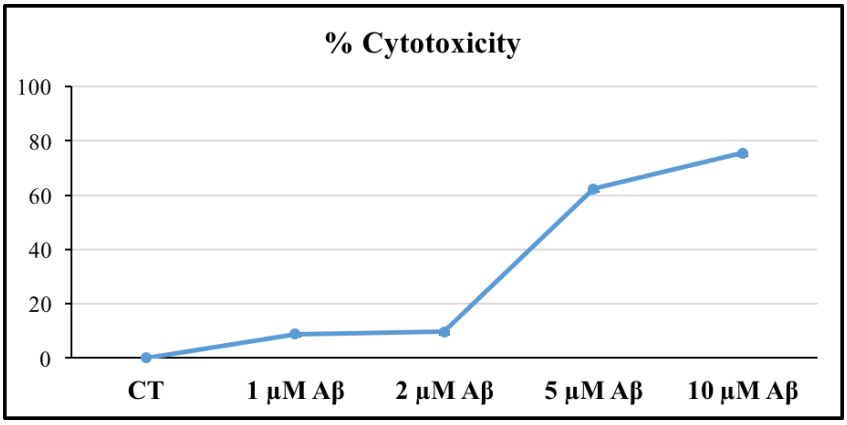


*Figure 32. LDH assay of SH-SY5Y cells exposed to an increasing concentration of Aβ oligomers allows to select the optimal concentration of oligomers that are cytotoxic for neuroblastoma cells.*

Data suggested that 200 nM of Hsp60 dramatically reduces Aβ-induced cytotoxicity, even though, at this concentration Hsp60 alone seems to be cytotoxic. A possible explanation of this phenomenon lays on the known role of Hsp60 in pro-death pathways [94] and therefore, if cannot be excluded that at lower concentrations Hsp60 is engaged in pro-apoptotic pathways. Consequently, other concentrations might be investigated to find an optimal concentration of Hsp60 that is well tolerated also in absence of Aβ oligomers.

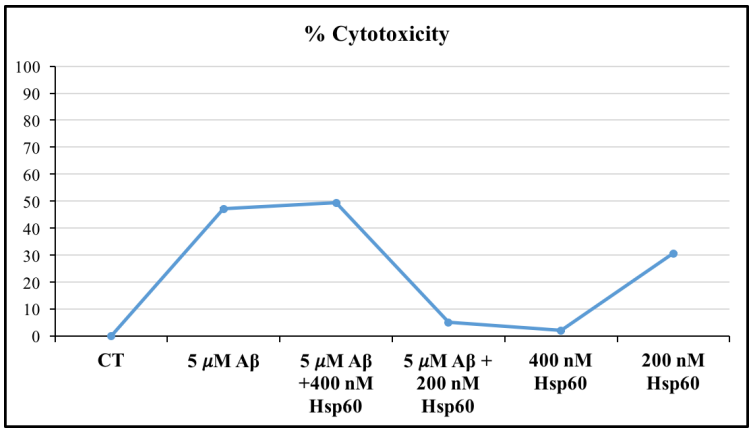


*Figure 33. LDH assay of SH-SY5Y cells exposed to different treatments (Aβ, Aβ + Hsp60 or Hsp60) suggests that Hsp60 can prevent Aβ toxicity in certain conditions.*

## 4. To determine Aβ and Hsp60 co-expression in *post mortem* tissues

Based on previous studies suggesting a relationship between the toxic accumulation of Aβ and impairment of chaperone levels in *post mortem* human tissues [121, 122], I characterized the co-expression of both proteins in total homogenates, synaptosomes and mitochondria by western blotting. Data summarized in figure 34 shows a representative WB in the left panel of total homogenates, mitochondria or synaptosomes isolated from either AD or age-matched controls, in the right panel the quantification of Hsp60 levels obtained by n=3 samples for each condition considered.

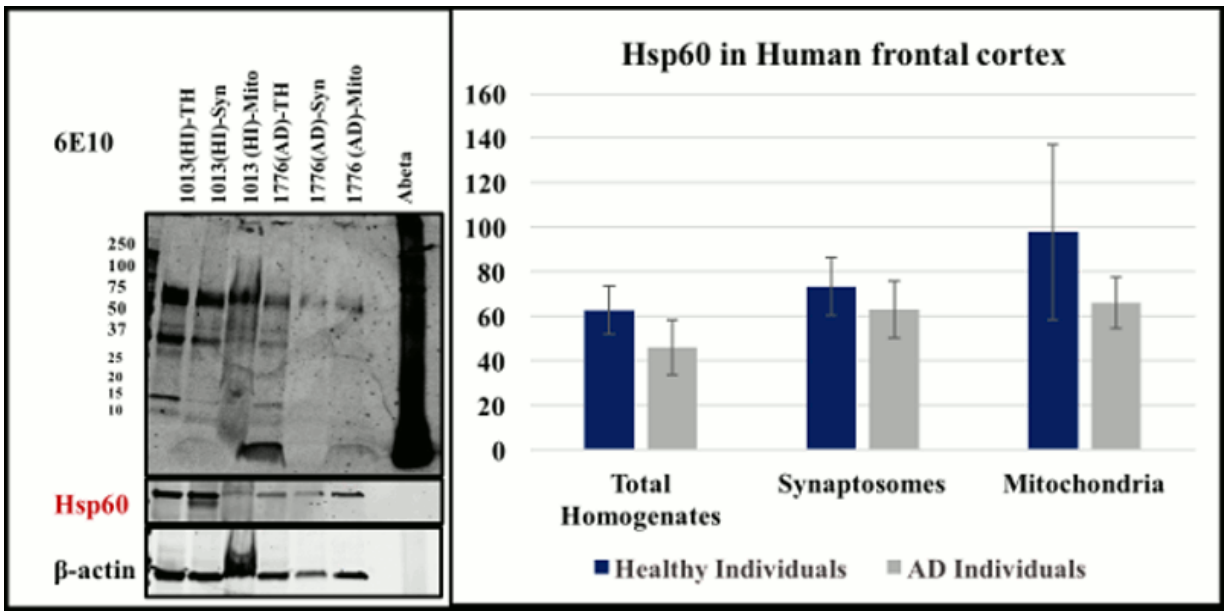


*Figure 34. Levels of Hsp60 by WB in AD individuals compared to healthy controls suggest a trend of reduction in AD patients. Hsp60 is particularly reduced in mitochondria compartment when comparing total homogenates, synaptosomes and mitochondria (n=3).*

Results obtained from Hsp60 quantification suggested a trend of reduction on Hsp60 levels in AD compared to controls. However, a larger number of sample will be required to test the working hypothesis is Hsp60 levels correlate with Aβ levels. Furthermore, a possible effect of the *post-mortem* interval on Hsp60 levels should also be taken into consideration.

## *Discussions*

AD is the 6th leading cause of death and this disease is going to increase its costs due to the absence of therapies [27]. One of the earliest hallmarks of AD pathogenesis is Aβ formation and aggregation into toxic oligomers that, together with the misfolding of other proteins, the impairment of the protein quality control machinery causes the disease. As Aβ neurotoxicity is one of the earliest events of the disease, this project aims to characterize a possible mechanism able to inhibit this toxicity. Based on what is the current knowledge on Aβ misfolding and aggregation pathway, there are several strategies that can be used to inhibit this process: to increase the clearance of Aβ oligomers and therefore to potentiate the removal of toxic species; to target toxic oligomers and readdress the aggregation cascade toward less toxic conformations; to target Aβ monomers, as soon as they are released, and directly inhibit the toxic "on-pathway" toward an trigger an alternative and less toxic "off-pathway".

Increasing research suggests that chaperones are protective machines that can counterbalance the toxic effect of other proteins [123-125]. Therefore, in my study I proposed to investigate the role of Hsp60 in interacting with Aβ peptide and I tested the potential protective effect against Aβ-induced neurotoxicity as a potential therapeutic strategy relevant to AD. In fact, to propose this chaperone as a backbone for any active therapy, it is crucial to define the mechanism of action, which so far is poorly understood.

The well characterized native properties of chaperonins Hsp60 in assisting the refolding of misfolded proteins, gave the rationale to propose a direct interaction between the two proteins. Therefore, I characterized the change in Aβ aggregation in presence of Hsp60 using Thioflavin T assay, circular dichroism spectroscopy, atomic force microscopy and size exclusion chromatography. I first investigated the effect of Hsp60 on Aβ aggregation by testing the protein-

protein interaction without the complexity of a cellular environment. Particularly, I confirmed that the mitochondrial form of human Hsp60 successfully inhibits the aggregation of either $A\beta_{1-40}$ and $A\beta_{1-42}$ peptides, using both Thioflavin T and circular dichroism analysis. Moreover, my data suggests that the machinery is acting also in absence of ATP, therefore I speculate that possibly Hsp60 offers a particularly hydrophobic surface that forces the aggregation of Aβ toward an "off-pathway" cascade, as after Hsp60 removal, the exposed amyloid peptide is not able to seed a new aggregation toward fiber formation a phenomenon already observed by others with fatty acids [126]. Moreover, the effect of Hsp60 in readdressing Aβ into an "off-pathway" seems irreversible, as purified Aβ exposed to Hsp60 loses the ability to aggregate even though exposed to pro-aggregating conditions. Moreover, data obtained with bacterial GroEL proposes that the possible mechanism of direct inhibition observed with the human homolog Hsp60 could be linked to a more evolved ability to operates also when the co-chaperone and ATP are not available, thus making this chaperone more evolved than the bacterial homologue GroEL.

As Hsp60 in a cell free model blocks Aβ aggregation and readdressed the amyloid pathway towards intermediates that have lost the ability to aggregate, I further investigated the effect of Hsp60 on Aβ production, compartmentalization and release by creating a novel cellular model that overexpresses both human amyloid precursor protein (APP) and human Hsp60 (referred as 7PA2/H60 cell line). This model supported the hypothesis that to overexpress Hsp60 protects against amyloid toxicity by reducing Aβ production as confirmed by ELISA of the extracellular media (conditioned media). Subsequently, I tested the effect of Hsp60 in inhibiting Aβ-driven cytotoxicity using SH-SY5Y cells as a neuronal model *in vitro*. Particularly, I tested the effect of Hsp60 on naturally secreted oligomers and preformed oligomers and tested the change in cytotoxicity compared to untreated oligomers. Overall, data suggests the protective action of Hsp60 against Aβ-driven cytotoxicity. Overall, data obtained can be summarized using the working model

summarized in figure 35. Briefly, Hsp60 targets either misfolded monomers or oligomers of Aβ, thus resulting in an irreversible inhibition of aggregation kinetic and the inhibition of Aβ-induce cytotoxicity as confirmed by data on neuroblastoma cell lines. Therefore, Hsp60 could be an attractive target for future therapies for Alzheimer's disease. Moreover, preliminary data obtained from *post mortem* tissues of AD brains, compared to healthy brains, suggested an impartment of Hsp60 levels that could be the outcome of an increased demand to counterbalance the aberrant production of toxic species responsible for AD pathogenesis.

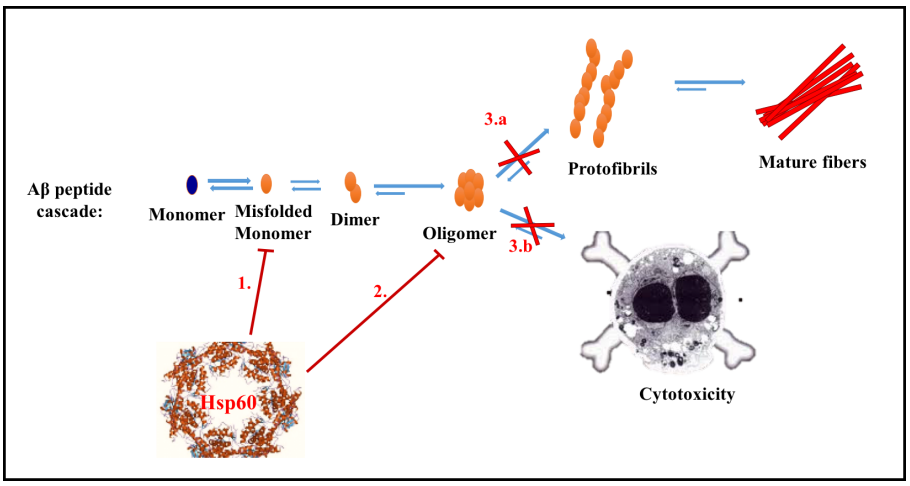


*Figure 35. Working model of the effect of Hsp60 on amyloid beta cascade and downstream toxicity.*

## *Conclusions*

Chaperones are an important component of the cellular protein quality control machinery. Increasing evidence suggests a direct interaction between chaperones and misfolded proteins characterizing several neurodegenerative diseases and proposes chaperones as protective guardians of cellular homeostasis [127, 128]. Alzheimer's disease is one example of neurodegenerative disorders, and often it has been defined by others as "protein misfolding pathology" [129, 130], as one of the hallmarks of the disease is Aβ formation and aggregation into neurotoxic forms leading to neurodegeneration. The aim of my project is to investigate the protective action of the mitochondrial chaperone Hsp60 against Aβ toxicity and proposes a novel approach against one of the causes of AD. Hsp60, as part of the protein quality control machinery, is known to protect the cell against stressors that alter cellular homeostasis. Moreover, there is evidence suggesting that Hsp60 might be involved in an aberrant circuitry triggered by amyloid misfolding and neurotoxicity [100]. Therefore, upregulating Hsp60, could contribute to prevent neurons to degenerate due to amyloid toxicity. Particularly, results in a cell free system highly suggest the inhibitory effect of Hsp60 on Aβ aggregation via an irreversible change in conformation of Aβ peptide. Moreover, *in vitro* results are highly suggestive that Hsp60 influences Aβ release, possibly due to a direct effect on APP processing or on sub-cellular localization thus resulting in a reduction of Aβ release in the extracellular compartment. Further investigations to better characterize the protective effect of Hsp60 *in vitro* might be needed to further confirm biochemistry of the process.

To test the effect of Hsp60 on Aβ cytotoxicity *in vitro,* suggests that Hsp60 significantly reduces the toxicity of both naturally secreted or preformed Aβ oligomers. Overall, the project contributes to characterize a poorly investigated mechanism of protection of the mitochondrial chaperonin

Hsp60 against Aβ toxicity, one of the main hallmarks of Alzheimer's disease and proposes Hsp60 as a potential key factor to consider for novel therapies.

## *Future directions*

Increasing evidence suggests that Aβ toxicity is due to specific oligomeric conformations (or "strains") acquired during Aβ aggregation kinetic [131, 132]. Therefore, any approach able to interfere with the formation of toxic oligomeric strains of Aβ is a successful strategy for future disease-modifying therapies. Using a cell free system, I showed that Hsp60 inhibits Aβ aggregation. Therefore, this data proposes Hsp60 as an effective inhibitor of *A*β aggregation. However, this study did not clarify what is the effect of Hsp60 on oligomeric strains of Aβ, which are known to have different neurotoxicity and to be the most relevant species for the onset of AD. Therefore, a future experiment will aim to test the working hypothesis that Hsp60 is responsible for inducing a change in Aβ oligomerization by changing its oligomeric strain toward less toxic species. To use specific antibodies against oligomeric conformation will provide evidence of the effect of Hsp60 on toxic Aβ strains.

To further validate the protective role of Hsp60 against amyloid-β toxicity, the protective effect of Hsp60 on Aβ neurotoxicity should be investigated also *in vivo*. In fact, to propose Hsp60 as a potential future therapy relevant to AD, should be confirmed if Hsp60 reverts some of the known phenotypes caused by Aβ toxicity: inhibition of the long-term potentiation and alteration of memory. In fact, this experiments will contribute to improve the understanding of the role of Hsp60 in AD and will provide a strong support for future therapeutics for AD.

Another interesting direction would be to investigate if there is a relationship between Hsp60 levels and the main risk factor responsible for the onset of sporadic AD, Apo Eε4, as the role in the onset of sporadic AD is poorly understood. An intriguing hypothesis lays on the recent discovery of a link between Apo E and clusterin [133], an extracellular chaperone known to be involved in cell survival and stress response and whose mechanism of action seems to be antagonized by a

direct binding to Hsp60 [134]. Interestingly, increased levels of clusterin have been associated with AD pathology and particularly with levels of APOE and increased secreted levels of tau and Aβ. Therefore, it would be interesting to test the hypothesis that the genetic variant Apo Eε4 has a role in influencing the chaperone machinery leading to a pathologic accumulation of pro-amyloid peptides, causing AD onset. The rationale that could support this hypothesis is the known interaction between ApoE, clusterin and Hsp60 [133,134]. A possible experimental approach could be to determine Hsp60 levels in transgenic mice expressing the human ApoE3, ApoE4 and ApoE2 variants and investigate if changes in Hsp60 levels might be indirectly influenced by increased levels in clusterin.

Another interesting aspect that might deserve further investigation concerns the observation that AD progression is linked to an impairment of inhibitory GABA neurons because of an accumulation of amyloid plaques, a phenomenon referred as "disinhibition" [135]. As the process seems to selectively involve a specifically GABA interneurons, it would be interesting to investigate both *in vivo* or *ex vivo* on animal models the hypothesis that this phenomenon of GABA-dependent disinhibition, leading to a "synaptic failure" characteristic of AD [136], could be influenced by an impairment of Hsp60 levels. To support this hypothesis will require functional studies using pharmacologic and electrophysiology approaches that will allow to test if to increase Hsp60 levels could compensate the impairment of GABAergic neurotransmission leading to aberrant firing and synaptic dysfunction.

## *References*


1. Strassning M. and Ganguli M. (2005) About a peculiar disease of the cerebral cortex: Alzheimer's original case revised. Psychiatry 2 (9): 30-33.

2. Kay D. W. K, Beamish P., and Roth M. (1964) Old age mental disorder in Newcastle-upon-Tyne. I. A study of prevalence. Br. J. Psychiatry 110:146–58.

3. Querfurth H. W. and La Ferla H. (2010) Alzheimer's disease. The New England Journal of Medicine 362: 329-44.

4. Annunziato L., Di Renzo G. F. et al. (2010) Trattato di Farmacologia. Idelson-Gnocchi (I Ed.).

5. Hardy J., Allsop D. (1991) Amyloid deposition as the central event in the etiology of Alzheimer's disease. Trends Pharmacol. Sci. 12: 383–388.

6. Braak H., Braak E. (1991) Neuropathological stageing of Alzheimer-related changes. Acta Neuropathol 82: 239-259.

7. Selkoe D. J. (2011) Alzheimer's disease. Cold Spring Harb. Perspect. Biol. 3 (7): a004457.

8. https://www.nia.nih.gov/alzheimers/publication/2011-2012-alzheimers-disease-progress-report/advances-detecting-alzheimers.

9. Sachdev P. S., Blacker D., Blazer D. G., Ganguli M., Jeste D. V., Paulsen J. S., Petersen R. C. (2014) Classifying neurocognitive disorders: the DSM-5 approach. Nat. Rev. Neurol. 10: 634–642.

10. Bjorklund N. L., Lindsay C. Reese, Sadagoparamanujam V-M, Ghirardi V., Woltjer R. L., Taglialatela G. (2012) Absence of amyloid β oligomers at the postsynapse and regulated synaptic Zn2+ in cognitively intact aged individuals with Alzheimer's disease neuropathology. Molecular Neurodegeneration 7:23.

11. Kramer P. L., Xu H., Woltjer R. L., Westaway S. K., Clark D., Erten-Lyons D., Kaye J. A., Welsh-Bohmer K. A., Troncoso J. C., Markesbery W. R., Petersen R. C., Turner R. S., Kukull W. A., Bennett D.A., Galasko D., Morris J. C., Ptt J. (2011) Alzheimer disease pathology in cognitively healthy elderly: A genome-wide study. Neurobiol. Aging 32:2113–2122.

12. Lue L. F., Kuo Y.M., Roher A.E., Brachova L., Shen Y., Sue L., Beach T., Kurth J. H., Rydel R. E., Rogers J. (1999) Soluble amyloid beta peptide concentration as a predictor of synaptic change in Alzheimer's disease. Am. J. Pathol. 155: 853–862.

13. Erten-Lyons D., Woltjer R. L., Dodge H., Nixon R., Vorobik R., Calvert J. F., Leahy M., Montine T., Kaye J. (2009) Factors associated with resistance to dementia despite high Alzheimer disease pathology. Neurology 72: 354–360.

14. Riudavets M. A., Iacono D., Resnick S. M., O'Brien R., Zonderman A. B., Martin L. J., Rudow G., Pletnikova O., Troncoso J. C. (2007) Resistance to Alzheimer's pathology is associated with nuclear hypertrophy in neurons. Neurobiol. Aging 28: 1484–1492.

15. Iacono D., O'Brien R., Resnick S. M., Zonderman A. B., Pletnikova O., Rudow G., An Y., West M. J., Crain B., Troncoso J. C. (2008) Neuronal hypertrophy in asymptomatic Alzheimer disease. J Neuropathol. Exp. Neurol. 67: 578–589.

16. Briley D., Ghirardi V., Woltjer R., Renck A., Zolochevska O., Taglialatela G., Micci M. A. (2016) Preserved neurogenesis in non-demented individuals with AD neuropathology. Sci. Rep. 6: 27812.

17. Cummings J., Aisen P. S., DuBois B., Frölich L., Jack C. R. Jr., Jones R. W., Morris J. C., Raskin J., Dowsett S. A., Scheltens P. (2016) Drug development in Alzheimer's disease: the path to 2025. Alzheimer's Research & Therapy 8: 39.

18. Schneider L. S., Sano M. (2009) Current Alzheimer's disease clinical trials: methods and placebo outcomes. Alzheimers Dement. 5: 388–97.

19. Masters C. L., Bateman R., Blennow K., Rowe C.C., Sperling R. A., Cummings J. L. (2015). Alzheimer's disease. Nat Rev. Dis. Primers 1: 15056.

20. Haass C., Kaether C., Thinakaran G., Sisodia S. (2012) Trafficking and proteolytic processing of APP. Cold Spring Harb. Perspect. Med. 2: a006270.

21. Epis R., Marcello E., Gardoni F., Di Luca M. (2012) Apha, beta- and gamma-secretases in Alzheimer's disease. Frontiers in bioscience S4: 1126-1150.

22. Musiek, E. S. and Holtzman D. M. (2015). Three dimensions of the amyloid hypothesis: time, space and 'wingmen'. Nat. Neurosci. 18(6): 800-806.

23. Herrup K. (2010) Re-imaging Alzheimer's disease- an age-based hypothesis. J. Neurosci. 30 (50): 16755-16762.

24. De Strooper B. (2010) Proteases and proteolysis in Alzheimer disease: a multifactorial view on the disease process. Physiol. Rev. 90, 465–494.

25. Taylor R.C. and Dillin A. (2011) Aging as an event of proteostasis collapse. Cold Spring Harb. Perspect. Biol. 3: a004440.

26. Lu T., Aron L., Zullo J., Pan Y., Kim H., Chen Y., Yang T. H., Kim H. M., Drake D. Liu X. S., Bennett D., A., Colaiacovo M. P., Yankner B. A. (2014) REST and stress resistance in ageing and Alzheimer's disease. Nature 507: 448–454.

27. Selkoe D. J. and Hardy J. (2016) The amyloid hypothesis of Alzheimer's disease at 25 years. EMBO Mol. Med. 8: 595-608.

28. Hirtz D., Thurman D. J., Gwinn-Hardy K., Mohamed M., Chaudhuri A. R., Zalutsky R. (2007) How common are the "common" neurologic disorders? Neurology 68: 326-37.

29. Dong H. K., Gim J. A., Yeo S. H., Kim H. S (2017) Integrated late onset Alzheimer's disease (LOAD) susceptibility genes: Cholesterol metabolism and trafficking perspectives. Gene 597:10-16.

30. Guerreiro R. and Hardy J. (2014) Genetics of Alzheimer's Disease. Neurotherapeutics 11, 732-737.

31. Karch C. M., Cruchaga C. and Goate A. M. (2014) Alzheimer's disease genetics: from the bench to the clinic. Neuron 83: 11-26.

32. Reitz C. and Mayeux R. (2014). Alzheimer disease: epidemiology, diagnostic criteria, risk factors and biomarkers. Biochem. Pharmacol. 88: 640-651.

33. Bertram L. and Tanzi R. (2012) The genetics of Alzheimer's disease. Prog. Mol. Biol. Transl. Sci. 107: 79–100.

34. Bruni A. C., Conidi, M. E. and Bernardi L. (2014) Genetics in degenerative dementia: current status and applicability. Alzheimer Dis. Assoc. Disord. 28: 199-205.

35. Kim J., Basak J.M. and Holtzman D.M. (2009) The role of apolipoprotein E in Alzheimer's disease. Neuron 63: 287-303.

36. Jarrett J.T., Berger E.P. and Lansbury Jr. P.T. (1993). The carboxy terminus of the beta amyloid protein is critical for the seeding of amyloid formation: Implications for the pathogenesis of Alzheimer's disease. Biochemistry 32: 4693-4697.

37. Yu C. E., Cudaback E., Foraker J., Thompson Z., Leong L., Lutz F., Gill J. A., Saxton A., Kraemer B., Navas P., Keene C. D., Montine T., Bekris L. M. (2013) Epigenetic signature and enhancer activity of the human APOE gene. Hum. Mol. Genet.: ddt354.

38. Weller R., Subash M., Preston S. D., Mazanti I., Carare R. O. (2008) Perivascular drainage of amyloid-b peptides from the brain and its failure in cerebral amyloid angiopathy and Alzheimer's disease. Brain Pathol. 18: 253-266.

39. Butterfield S., Hejjaoui M., Fauvet B., Awad L., Lashuel H. A. (2012) Chemical strategies for controlling protein folding and elucidating the molecular mechanisms of amyloid formation and toxicity. JMB 421: 204-36.

40. Soto C. (2003) Unfolding the role of protein misfolding in neurodegenerative diseases. Nature Reviews 4: 49-60.

41. Kang J., Lemaire H. G., Unterbeck A., Salbaum J. M., Masters C. L., Grzeschik K. H., Multhaup G., Beyreuther K., Müller-Hill B. (1987) The precursor of Alzheimer's disease amyloid A4 protein resembles a cell-surface receptor. Nature 325 (19): 733-36.

42. Haass C., Kaether C., Thinakaran G., Sisodia S. (2012) Trafficking and proteolysis processing of APP. Cold Spring Arb. Perspective Med. 2: a006270.

43. Haass C. (2004). Take five-BACE and the gamma secretase quartet conduct Alzheimer's amyloid beta-peptide generation. EMBO J 23: 483-88.

44. Querfurth H. W. and La Ferla F. M. (2010) Alzheimer's Disease. New England Journal of Medicine 362 (4): 329-44.

45. Bodani R. U., Sengupta U., Castillo-Carranza D. L., Guerrero-Muñoz M. J., Gerson J., Rudra J., Kayed R. (2015) Antibody against small aggregated peptide specifically recognizes toxic Aβ-42 oligomers in Alzheimer's disease. ACS Chem. Neurosci. 6: 1981-89.

46. Jarrett J. T. and Lansbury P. T. (1993) Seeding "one-dimensional crystallization" of amyloid: a pathogenic mechanism in Alzheimer's disease and scrapie? Cell 73: 1055-58.

47. Kumar S. and Walter J. (2011) Phosphorylation of amyloid beta peptides – A trigger for formation of toxic aggregates in Alzheimer's disease. Aging 3 (8): 1-10.

48. Fändrich M., Schmidt M., Grogorieff N. (2011) Recent progress in understanding Alzheimer's β-amyloid structures. Trends Biochem. Sci. 36 (6): 338-345.

49. Necula M., Kayed R., Milton S., Glabe C. G. (2007) Small molecule inhibitors of aggregation indicate that amyloid β oligomerization and fibrillation pathways are independent and distinct. JBC 282 (14): 10311-24.

50. Hsia A. Y., Masliah E., Mc Conlogue L., Yu G. Q. (1999) Tatsuno, G., Hu, K., Kholodenko, D., Malenka R. C., Nicoll R. A., and Mucke L. Plaque-independent disruption of natural circuits in Alzheimer's disease mouse models. Proc. Natl. Acad. Sci. USA 96: 3228-3233.

51. Kayed R., Canto I., Breydo L., Rasool S., Lukacsovich T., Wu J., Albay R. 3rd, Pensalfini A., Yeung S., Head E., Marsh J. L., Glabe C. (2010) Conformation dependent monoclonal antibodies distinguish different replicating strains or conformers of prefibrillar Abeta oligomers. Mol. Neurodegener. 5: 57.

52. Tomic J. L., Pensalfini A., Head E., and Glabe C. G. (2009) Soluble fibrillar oligomer levels are elevated in Alzheimer's disease brain and correlate with cognitive dysfunction. Neurobiol. Dis. 35, 352−358.

53. Dineley K. T., Kayed R., Neugebauer V., Fu Y., Zhang W., Reese L. C., Taglialatela G. (2010) Amyloid beta oligomers impair fear conditioned memory in a calcineurin-dependent fashion in mice. J. Neurosci. Res. 88 (13): 2923-2932.

54. Kayed R. and Lasagna-Reeves C. A. (2013) Molecular mechanisms of amyloid oligomers toxicity. J. Alzheimer's Dis. 33 (Suppl. 1), S67−78.

55. Kayed R., Head E., Thompson J. L., Mclntire T. M., Milton S. C., Cotman C. W., Glabe C. G. (2003). Common structure of soluble amyloid oligomers implies common mechanism of pathogenesis. Science 300 (5618): 486-489.

56. Nowles T.P., Vendruscolo M., Dobson C.M. (2014) The amyloid state and its association with protein misfolding diseases. *Nat. Rev. Mol. Cell Biol.* **15**:384–396.

57. Ries H. M. and Nussbaum-Krammer C. (2016) Shape matters: the complex relationship between aggregation and toxicity in protein-misfolding diseases. Essays in Biochemistry 60(2): 181-190.

58. Braak H. and Del Tredici K. (2011) Alzheimer's pathogenesis: is there neuron-to-neuron propagation? Acta Neuropathol. 121: 589-595.

59. Cai Q. and Tammineni P. (2016) Mitochondrial aspects of synaptic dysfunction in Alzheimer's disease. J. Alzheimer's Disease. E. pub ahead of print.

60. Lustbader J.W., Cirilli M., Lin C., Xu H. W., Takuma K., Wang N., Caspersen C., Chen X., Pollak S., Chaney M., Trinchese F., Liu S., Gunn-Moore F., Lue L. F., Walker D. G., Kuppusamy P., Zewier Z. L., Arancio O., Stern D., Yan S. S., Wu H. (2004) ABAD directly links Abeta to mitochondrial toxicity in Alzheimer's disease. Science 304: 448-452.

61. Manczak M., Mao P., Calkins M.J., Cornea A., Reddy A. P., Murphy M. P., Szeto H. H., Park B., Reddy P. H. (2010) Mitochondria-targeted antioxidants protect against amyloid-beta toxicity in Alzheimer's disease neurons. J. Alzheimer's Dis. 20 (Suppl. 2): S609-S631.

62. Spires-Jones T. L. and Hyman B. T. (2014) The intersection of amyloid beta and tau at synapses in Alzheimer's disease. Neuron 82 (4): 746-771.

63. Spillantini M, Goedert M. (2013) Tau pathology and neurodegeneration. Lancet neurology 12: 609–622.

64. Hickman R. A., Faustin A., Wisniewski T. (2016) Alzheimer's disease and its growing epidemic. Neurol. Clin. 34: 941-53.

65. Reddy P. H. and Mc Weeney S. (2006) Mapping cellular transcriptosomes in autopsied Alzheimer's disease subjects and relevant animal models. Neurobiol. Aging 27, 1060–1077.

66. Reddy P. H. and Beal M. F. (2007) Amyloid beta, mitochondrial dysfunction and synaptic damage: implications for cognitive decline in aging and Alzheimer's disease. Trends in molecular medicine 14 (2): 45-53.

67. Frautschy S. A., Cole G. M. (2010) Why pleiotropic interventions are needed for Alzheimer's disease. Mol. Neurobiol. 41:392–409.

68. Mattson M. P. (2006) Molecular and cellular pathways towards and away from Alzheimer's disease. In: Jucker M., Beyreuther K., Haass C., Nitsch R., Christen Y. (eds.) Alzheimer: 100 years and beyond. Springer, Berlin: 371–378.

69. Morimoto R. I. and Cuervo A. M. (2009) Protein homeostasis and aging: taking care of proteins from the cadle to the grave. J. Geront. A Biol. Sci. Med. Sci. 64 A (2): 167-170.

70. Farlow M. R., Salloway S., Tariot P. N., Yardley J., Moline M. L., Wang Q., Brand-Schieber E., Zou H., Hsu T., Satlin A. (2010) Effectiveness and tolerability of high-dose (23 mg/d) versus standard-dose (10 mg/d) donepezil in moderate to severe Alzheimer's disease: a 24-week, randomized double-blind study. Clinical therapeutics 32 (7): 1234-51.

71. Brunton L., Chabner B., Knollman B. (2012) Goodman and Gilman's the pharmacological basis of therapeutics, 12th edition.

72. Ritter A. and Cummings J. (2015) Fluid biomarkers in clinical trials of Alzheimer's disease therapeutics. Front. Neurol. 6: 186.

73. Singh B., Patel H. V., Ridley R. G., Freeman K. B., Gupta R. S. (1990) Mitochondrial import of the human chaperonin (hsp60) protein. Biochemical and biophysical research communications 169 (2): 391-396.

74. Douglas P. M. and Dillin A. (2010) Protein homeostasis and aging in neurodegeneration. J. Cell. Biol. 190 (5): 719-29.

75. Macario A. J., Cappello F., Zummo G., Conway de Macario E. (2010) Chaperonopathies of senescence and the scrambling of interactions between the chaperoning and the immune system. Ann. N. Y. Acad. Sci. 1197: 85-93.

76. Ellis R. J. (1987) Proteins as molecular chaperones. Nature 328: 378 – 379.

77. Richter K., Haslbeck M., Buchner J. (2010) The heat shock response: life on the verge of death, Mol. Cell 40: 253–266.

78. Skjærven L., Cuellar J. C., Martinez A., Valpuesta J. M. (2015) Dynamics, flexibility, and allosteric properties in molecular chaperonins. FEBS Letters 589: 2522-32.

79. Ellis R. J. (2006) Molecular chaperones: assisting assembly in addition to folding, Trends Biochem. Sci. 31:395–401.

80. Kim Y. E., Hipp M. S., Bracher A., Hayer-Hartl M., Hartl F. U. (2013) Molecular chaperone functions in protein folding and proteostasis. Annu. Rev. Biochem. 82: 323-55.

81. Chaudhuri, T.K., Farr, G.W., Fenton, W.A., Rospert. S. and Horwich, A.L. (2001). GroEL/GroES-mediated folding of a protein too large to be encapsulated. Cell 107, 235-246.

82. Uversky V. N. (2011) Intrinsically disordered chaperones and neurodegeneration, in: S.N. Witt (Ed.), Protein Chaperones and Protection from Neurodegenerative Diseases, Wiley.

83. Uversky V. N., Gillespie J. R., Fink A. L. (2000) Why are "natively unfolded" proteins unstructured under physiologic conditions? Proteins 41 (3): 415-27.

84. Tompa, P. and Csermely, P. (2004) The role of structural disorder function in the function of RNA and protein chaperones. FASEB J. 18: 1169-75.

85. Kovacs B., and Tompa P. (2012) Diverse functional manifestations of intrinsic structural disorder in molecular chaperones. Biochem. Soc. Trans. 40 (5):963-8.

86. Dunker A. K., Brown C. J. Obradovic Z. (2002) Identification and functions of usefully disordered proteins. Ad V. Protein. Chem. 62: 25-49.

87. Xu Z., Horwich A.L. and Sigler P.B. (1997) The crystal structure of the asymmetric GroEL–GroES–(ADP)7 chaperonin complex. Nature 388, 741–750.

88. Braig, K., Otwinowski, Z., Hegde, R., Boisvert, D.C., Joachimiak, A., Horwich, A.L., Sigler, P.B. (1994) The crystal structure of the bacterial chaperonin GroEL at 2.8 Å. Nature 371, 578–586.

89. Okamoto T., Ishida R., Yamamoto H., Tanabe-Ishida M., Haga A., Takahashi H., Takahashi K., Goto D., Grave E., Itoh H. (2015) Functional structure and physiological functions of mammalian wild-type Hsp60. Arch. Biochem. Biophys. 586: 10-9.

90. Ellis R. J. (2003) Protein folding: importance of the Anfinsen cage. Curr. Biol. 13: R881–R883.

91. Barral J. M., Broadley S. A., Schaffar G., Hartl F. U. (2004) Roles of molecular chaperones in protein misfolding diseases. Seminars in cell & developmental biology 15: 17-29.

92. Bigotti M.G. and Clarke A.R. (2008) Chaperonins: the hunt for the Group II mechanism. Arch. Biochem. Biophys. 474, 331–339.

93. Cheng M.Y., Hartl F.U., Horwich A.L. (1990) The mitochondrial chaperonin Hsp60 is required for its own assembly. Nature 348: 455–458.

94. Chandra D., Choy G. and Tang D. G. (2007) Cytosolic accumulation of Hsp60 during apoptosis with or without apparent mitochondrial release. JBC 282 (43):31289-301.

95. Cappello F., Conway De Macario E., Marasa` L., Zummo G. (2008) Hsp60 expression, new locations, functions and perspectives for cancer diagnosis and therapy. Cancer Biology & Therapy 7 (6): 801-809.

96. Bigotti M.G. and Clarke, A.R. (2008) Chaperonins: the hunt for the Group II mechanism. Arch. Biochem. Biophys. 474, 331–339.

97. Balchin D., Hayer-Hartl M., Hartl F. U. (2016) In vivo aspects of protein folding and quality control. Science 353: aac4354.

98. Asea A. A. A. (2008) Heat Shock proteins and the brain: Implications for neurodegenerative diseases and neuroprotection. Springer Ed.

99. Veereshwarayya V., Kumar P., Rosen K. M., Mestril R., Querfurth H. W. (2006) Differential effects of mitochondrial heat shock protein 60 and related molecular chaperones to

prevent intracellular beta-amyloid-induced inhibition of complex IV and limit apoptosis. J. Biol. Chem. 281: 29468–29478.

100. Walls K. C., Coskun P., Gallegos-Perez J. L., Zadourian N., Freude K., Rasool S., Blurton-Jones M., Green K. N., La Ferla F. M. (2012) Swedish Alzheimer mutation induces mitochondrial dysfunction mediated by HSP60 mislocalization of amyloid precursor protein (APP) and beta-amyloid, J. Biol. Chem. 287: 30317–30327.

101. Morley J. F., Brignull H. R., Weyers J. J., Morimoto R.I. (2002) The threshold for polyglutamine-expansion protein aggregation and cellular toxicity is dynamic and influenced by aging in Caenorhabditis elegans. Proc. Natl. Acad. Sci. USA 99:10417–22.

102. Fezoui Y., Hartley D. M., Harper J. D., Khurana R., Walsh D. M., Condron M. M., Selkoe D. J., Lansbury P. T., Fink A. L., Teplow D. B. (2000) An improved method of preparing the amyloid beta-protein for fibrillogenesis and neurotoxicity experiments. Amyloid 7: 166–178.

103. Lakowicz, J. R. (2006) Principles of fluorescence spectroscopy, 3° Ed.

104. Carrotta R., Di Carlo M., Manno M., Montana G., Picone P., Romancino D., San Biagio P. L. (2006) Toxicity of recombinant beta-amyloid prefibrillar oligomers on the morphogenesis of the sea urchin Paracentrotus lividus. FASEB J. 20 (11): 1916–1927.

105. Wolfe L. S., Calabrese M. F., Nath A., Blaho D. V., Miranker A. D., Xiong Y. (2010) Protein-induced photophysical changes to the amyloid indicator dye Thioflavin T. Proc. Natl. Acad. Sci. USA 107 (39):16863-8.

106. Mangione M.R., Vilasi S., Marino C., Librizzi F., Canale C., Spigolon D., Fucarino A., Passantino R., Cappello F., Bulone D. San Biagio P. L. (2016) Hsp60, amateur chaperon in amyloid-beta fibrillogenesis. BBA- General subjects 1860 (11): 2474-2483.

107. Van Holde K. E., Curtis Johnson W., Shing Ho P. (1999) Principles of Physical Biochemistry. Prentice Hall. 2nd Edition.

108. Meli G., Lecci A., Manca A., Krako N., Albertini V., Benussi L., Ghidoni R., Cattaneo A. (2014) Conformational targeting of intracellular Aβ oligomers demonstrates their pathological oligomerization inside the endoplasmic reticulum. Nature Communications 5: 3867.

109. Dunstan D. E., Hamilton-Brown P., Asimakis P., Ducker W., Bertolini J., (2009) Shear flow promotes amyloid-β fibrilization. PEDS 22: 741–746.

110. Hamilton-Brown P., Bekard I., Ducker W.A., D.E. Dunstan. (2008) How does shear affect Aβ fibrillogenesis? J. Phys. Chem. B 112: 16249–16252.

111. https://tools.thermofisher.com/content/sfs/manuals/Lipofectamine_2000_Reag_protocol.pdf.

112. Yagi-Utsumi M. and Dobson C. M. (2015) Conformational effects of the A21G Flemish mutation on the aggregation of Amyloid β peptide. Biol. Pharm. Bull. 38: 1668-72.

113. Cukalevski R., Boland B., Frohm B., Thulin E., Walsh D., Linse S. (2012) Role of aromatic side chains in amyloid β-protein aggregation. ACS Chem. Neurosci. 3(12):1008-16.

114. Garvey M. and Morgado I. (2013) Peptide concentration alters intermediate species in amyloid β fibrillation kinetics. Biochem. Biophys. Res. Commun. 433(3):276-80.

115. Hellstrand E., Boland B., Walsh D., Linse S., Amyloid beta-protein aggregation produces highly reproducible kinetic data and occurs by a two-phase process, ACS Chem. Neurosci. 1 (2010) 13–18.

116. Podlisny M. B., Ostaszewski B. L., Squazzo S. L., Koo E. H., Rydell R. E., Teplow D. B., and Selkoe, D. J. (1995) Aggregation of secreted amyloid beta-protein into sodium dodecyl sulfate-stable oligomers in cell culture. J. Biol. Chem. 270, 9564-957.

117. Walsh D. M., Klyubin I., Fadeeva J. C., Cullen W. K., Anmyl R., Wolfe M. S., Rowan M. J., Selkoe D. J. (2002). Naturally secreted oligomers of amyloid β-protein potently inhibit hippocampal long term potentiation in vivo. Nature, 416: 535-9.

118. Manczak M., Anekonda T. S., Henson E., Park B. S., Quinn J., Reddy P. H. (2006) Mitochondria are a direct site of Abeta accumulation in Alzheimer's disease neurons: Implications for free radical generation and oxidative damage in disease progression. Hum. Mol. Genet. 15, 1437-1449.

119. Tillement L., Lecanu L., Papadopoulos V. (2011) Alzheimer's disease: effects of β-amyloid on mitochondria. Mitochondrion 11 (1): 13-21.

120. Welzel A. T., Maggio J. E., Shankar G. M., Walkar D. E., Ostaszewski B. L., Li S., Klyubin I., Rowan M. J., Seubert P., Walsh D. M., Selkoe D. J. (2014) secreted amyloid β-proteins in a cell culture model include N-terminally extended peptides that impair synaptic plasticity. Biochemistry 53 (24): 3908-21.

121. Calabrese V., Sultana R., Scapagnini G., Guagliano E., Sapienza M., Bella R., Kanski J., Pennisi G., Mancuso C., Giuffrida Stella A. M., Butterfield D. A. (2006) Nitrosative stress, cellular stress response and thiol homeostasis in patients with Alzheimer's disease. Antioxidants & Redox signaling 8 (11):1975-86.

122. Di Domenico D., Sultana R., Tiu G. F., Scheff N. N. Perluigi M., Cini G., Butterfield D. A. (2010) Protein levels of Heat Shock proteins 27, 32, 60, 70, 90 and Thioredoxin-1 in Amnestic mild cognitive impairment: an investigation on the role of cellular stress response in the progression of Alzheimer's disease. Brain Res. 1333:72-81.

123. Cortez L. and Sim V. (2014) The therapeutic potential of chemical chaperones in protein folding diseases. Prion 8 (2): 197-202.

124. Tanaka M., Machida Y., Niu S., Ikeda T., Jana N. R., Doi H., Kurosawa M., Nekooki M., Nukina N. (2004) Trehalose alleviates polyglutamine-mediated pathology in a mouse model of Huntington disease. Nat Med 10:148-54.

125. Cox D., Selig E., Griffin M.D., Carver J. A., Ecroyd H. (2016) Small heat shock proteins prevent α-synuclein aggregation via transient interactions and their efficacy is affected by the rate of aggregation. J. Biol. Chem. 29 (43): 22616-629.

126. Kumar A., Paslay L. C., Lyons D., Morgan S. E., Correia J. J., Rangachari V. (2012) Specific soluble oligomers of amyloid-β peptide undergo replication and form non-fibrillar aggregates in interfacial environment. J. Biol. Chem. 287 (25): 21253-64.

127. Morimoto R. I. and Cuervo A. M. (2014) Proteostasis and the aging proteome in health and disease. J. Gerontol. A Biol. Sci. Med. Sci. 69 (S1): S33-S38.

128. Hartl F. U., Bracher A., Hayer-Hartl M. (2011) Molecular chaperones in protein folding and proteostasis. Nature 475 (7356): 324-32.

129. Khanam H., Ali A., Asif M., Shamsuzzaman (2016) Neurodegenerative diseases linked to misfolded proteins and their therapeutic approaches: A review. Europ. J. Med. Chem. 124: 1121-41.

130. Ugalde C. L., Finkelstein D. I., Lawson V. A., Hill A. F. (2016) Pathogenic mechanisms of prion protein, amyloid-β and α-synuclein misfolding: the prion concept and neurotoxicity of protein oligomers. J. Neurochem. 139 (2): 162-80.

131. Liu P., Reed M. N., Kotilinek L. A., Grant M. K. O., Forster C. L., Qiang W., Shapiro S. L., Reichl J. H., Chiang A. C. A., Jankowsky J. L., Wilmot C. M., Cleary J. P., Zahs K. R. (2015) Quaternary structure defines a large class of amyloid-β oligomers neutralized by sequestration. Cell. Rep. 11 (11): 1760-71.

132. Bao F., Wicklund L., Lacor P. N., Klein W. L., Nordberg A., Marutle A. (2012) Different β-amylid oligomer assemblies in Alzheimer brains correlate with age of disease onset and impaired cholinergic activity. Neurobiology of Aging 33: 825.e1-825.e13.

133. Deming Y., Xia J., Cai Y., Lord J., Holmans P., Bertelsen S., Alzheimer's disease Neuroimaging Initiative (ADNI), David Holtzman, Morris J. C., Bales K., Pickering E. H., Kauwe J., Goate A., Cruchaga C. (2016) A potential endophenotype for Alzheimer's disease: cerebrospinal fluid clusterin. Neurobiol. Aging 37: 208.e1-e9.

134. Chaiwatanasirikul K. A. and Sala A. (2011) The tumor-suppressive function of CLU is explained by its localization and interaction with Hsp60. Cell Death and Disease 2, e219.

135. Busche M. A., Eichhoff G., Adelsberger H., Abramowski D., Wiederhold K. H., Haass C., Staufenbiel M., Konnerth A., Garaschuk O. (2008) Clusters of hyperactive neurons near amyloid plaques in a mouse model of Alzheimer's disease. Science 321 (5896): 1686-9.

# *List of abbreviations*

AD = Alzheimer's disease

Aβ = amyloid beta

APP = amyloid precursor protein

CSF = cerebral spinal fluid

NDAN = Non-Demented with Alzheimer's Neuropathology

fAD = familiar Alzheimer's disease

sAD = sporadic Alzheimer's disease

BACE1 = beta-secretase 1

MW = molecular weight

IDRs = intrinsically disordered regions

Hsp6 0 = Heat shock protein

AFM = Atomic force microscopy

HFIP = Hexafluoro-2-propanol

ThT = Thioflavin T

CD = Circular Dichroism

HPLC= High performance liquid chromatography

SEC= Size exclusion chromatography

CHO = Chinese Hamster Ovary

7PA2 = CHO overexpressing $APP_{swe}$ protein

7PA2/H60= 7PA2 overexpressing Hsp60

DMEM = Dulbecco's modified Eagle Medium

FBS = Fetal bovine serum

CM= Conditioned Medium

WB = Western blotting

PBS = Phosphate buffer saline

ICC = Immunocytochemistry

IP = Immuno-precipitation

LDH= Lactate Dehydrogenase